Development 139, 3600-3612 (2012) doi:10.1242/dev.081786

The E3 ligase Cdh1-anaphase promoting complex operates upstream of the E3 ligase Smurf1 in the control of axon growth

Madhuvanthi Kannan, Shih-Ju Lee, Nicola Schwedhelm-Domeyer and Judith Stegmüller*

SUMMARY

Axon growth is an essential event during brain development and is extremely limited due to extrinsic and intrinsic inhibition in the adult brain. The E3 ubiquitin ligase Cdh1-anaphase promoting complex (APC) has emerged as an important intrinsic suppressor of axon growth. In this study, we identify in rodents the E3 ligase Smurf1 as a novel substrate of Cdh1-APC and that Cdh1 targets Smurf1 for degradation in a destruction box-dependent manner. We find that Smurf1 acts downstream of Cdh1-APC in axon growth and that the turnover of RhoA by Smurf1 is important in this process. In addition, we demonstrate that acute knockdown of Smurf1 in vivo in the developing cerebellar cortex results in impaired axonal growth and migration. Finally, we show that a stabilized form of Smurf1 overrides the inhibition of axon growth by myelin. Taken together, we uncovered a Cdh1-APC/Smurf1/RhoA pathway that mediates axonal growth suppression in the developing mammalian brain.

KEY WORDS: Cdh1-APC, Smurf1, Axon growth, Myelin, Ubiquitylation, Mouse, Rat

INTRODUCTION

Axon growth is a crucial process in the developing nervous system. It is controlled by a large number of extrinsic regulatory events, which trigger signaling cascades that involve small GTPase-controlled reorganization of the cytoskeleton (Dent and Gertler, 2003; Dickson, 2001; Huber et al., 2003). By contrast, little is known about how intrinsic mechanisms, including the ubiquitin proteasome system (UPS), act from within the neurons to control axon growth.

Components of the UPS comprise E1 and E2 enzymes and E3 ubiquitin ligases, which mediate the transfer of ubiquitin to substrate proteins and thus trigger different events ranging from proteasome-mediated degradation to functional modification of the substrate (Hershko and Ciechanover, 1998). The UPS regulates different cellular events and has emerged as a crucial regulator of brain development (Kawabe and Brose, 2011; Stegmüller and Bonni, 2010; Yi and Ehlers, 2007). An estimated 600 E3 ligases are responsible for the recruitment and ubiquitylation of an even larger number of substrates (Nalepa et al., 2006).

The E3 ubiquitin ligase Cdh1-anaphase promoting complex (APC) is a well-known regulator of mitosis. By recruiting substrates to the APC core, Cdh1 targets several proteins for proteasomal degradation to ensure cell cycle transition (Harper et al., 2002; Peters, 2002). Beyond the cell cycle, Cdh1-APC has been implicated in fundamental functions of the brain including glial migration, axon growth, synaptic development, neuronal glycolysis, survival, and learning and memory (Almeida et al., 2005; Herrero-Mendez et al., 2009; Juo and Kaplan, 2004; Konishi et al., 2004; Kuczera et al., 2011; Li et al., 2008; Silies and Klämbt, 2010; van Roessel et al., 2004). In axon growth control, Cdh1-APC mediates intrinsic suppression by targeting the transcriptional regulators SnoN and Id2 for degradation (Ikeuchi et al., 2009; Lasorella et al., 2006; Stegmüller et al., 2006). Whereas SnoN acts together with Smad2 and upstream of the scaffold protein Ccd1 in axon growth control, Id2 regulates gene implicated in axon growth inhibition e.g. the Nogo receptor gene (Lasorella et al., 2006; Stegmüller et al., 2008). Strikingly, knockdown of Cdh1 stimulates axon growth in the presence of myelin, a well-known inhibitor of axon outgrowth and regeneration (Hu and Strittmatter, 2004; Konishi et al., 2004; Schwab, 2004). Myelin-induced inhibition is exerted by binding of myelin proteins to the neuronal Nogo receptor complex, triggering signaling cascades, which converge on the key signaling component RhoA (Fournier et al., 2003; Giger et al., 2010; McGee and Strittmatter, 2003; Schwab, 2004; Yiu and He, 2006). Since Cdh1-APC controls several substrates in cell cycle regulation, we reasoned that Cdh1-APC-mediated intrinsic axon growth would be of similar complexity and require multi-substrate regulation. Thus, in addition to SnoN and Id2, Cdh1-APC might regulate other components of axon growth inhibition. We hypothesized that Cdh1-APC might directly or indirectly affect RhoA, as RhoA plays a crucial role in inhibiting axon growth and is a key component of myelin inhibition (Fournier et al., 2003; Govek et al., 2005).

In this study, we identified the RhoA-regulating E3 ligase Smurf1 as a novel substrate of Cdh1-APC and characterized the Cdh1-APC/Smurf1/RhoA pathway of axon growth regulation.

MATERIALS AND METHODS

Plasmids and reagents

The RhoA, SnoN DBM and Id2 DBM expression plasmids have been described previously (Coso et al., 1995; Lasorella et al., 2006; Stegmüller et al., 2006). The HA-Smurf1 DBMs 1-5, DBM3/4 and rescue plasmid and the RhoA K6,7R plasmid (Ozdamar et al., 2005) were generated by site-directed mutagenesis. The HA-NES-Smurf1 and HA-NLS-Smurf1 rescue plasmids were constructed by introducing two tandem repeats of HIV-1 *Rev* nuclear export signal and SV40 large T-antigen nuclear localization signal (Yoneda et al., 1999), respectively, into the pCMV5-HA-Smurf1

MPI of Experimental Medicine, Hermann Rein Strasse 3, 37075 Göttingen, Germany.

*Author for correspondence (stegmueller@em.mpg.de)

Accepted 11 July 2012

rescue plasmid. In addition, the internal nuclear export signal in Smurf1 (Tajima et al., 2003) was mutated (I612A, L614A) in the HA-NLS-Smurf1 rescue plasmid. The Cdh1 RNAi plasmid has been described previously (Konishi et al., 2004). The Smurf1 RNAi plasmid was generated by cloning a previously described Smurf1 RNAi sequence (Boyer et al., 2006) into a modified pBluescript-U6 plasmid.

In vivo electroporation

In vivo electroporation was performed as described previously (Stegmüller et al., 2006). Briefly, plasmid DNA in PBS (3-4 μl/animal) together with 0.3% Fast Green was injected into the cerebellar cortex of P4 Wistar rat pups using a Hamilton syringe with a 30-gauge needle. U6-CMV-EGFP or U6/Smurf1-CMV-EGFP plasmids were injected at 4 μg/μl and Bcl-xl expression vectors at 1 μg/μl. Following DNA injection, animals were subjected to electric pulses (five pulses of 160-170 V for 50 mseconds with intervals of 950 mseconds). The electroporated pups were sacrificed 5 days later. The cerebella were sectioned (40 μm) in a Leica cryostat and subjected to immunohistochemistry with GFP antibody (1:500; Santa Cruz Biotechnology, Santa Cruz, CA, USA). In control U6-CMV-GFP cerebella we typically found a 90% association of GFP-positive granule neurons with parallel fibers: the parallel fiber index (Stegmüller et al., 2006). All experiments involving live animals were conducted according to animal protocols approved by the Verbraucherschutz und Lebensmittelsicherheit of Lower Saxony, Germany.

Primary neuron culture and transfections

Granule neurons were isolated from Wistar rats at postnatal day (P) 6 as described previously (Konishi et al., 2002). Neurons were plated on polyornithine-coated glass coverslips and kept in Basal Medium Eagle (BME; Invitrogen, Carlsbad, CA, USA) supplemented with 10% calf serum (Hyclone Laboratories, Logan, UT, USA), 25 mM KCl and 2 mM penicillin, streptomycin and glutamine (PSG), or with glucose, PSG and 10 μg/ml insulin. At P6 plus 1 day in vitro (DIV), neurons were treated with 10 μM cytosine β-D-arabinofuranoside, a mitotic inhibitor, to prevent the proliferation of non-neuronal cells.

Granule neurons were transfected 8 hours after plating and cortical neurons at DIV 1 using the modified calcium phosphate method with the indicated plasmids together with a GFP expression plasmid to visualize transfected neurons. To rule out any effect of the genetic manipulations on cell survival, the anti-apoptotic protein Bcl-xl was co-expressed in all the experiments. The expression of Bcl-xl itself has little or no effect on axon length (Konishi et al., 2004). Neurons on 12-mm coverslips were transfected with a total of 2 μg of plasmid together with 0.3 μg Bcl-xl and 0.2 μg of GFP expression plasmid. The control plasmid for each transfection was the respective empty vector. The transfection ensures that more than 85% of the GFP-positive neurons co-express two other plasmids.

Cultured neurons were fixed in 4% formaldehyde at DIV 3 or DIV 4 and subjected to immunocytochemistry with GFP antibody (1:1000; Invitrogen). Cultured neurons were subjected to immunocytochemistry with a Smurf1 antibody (Sigma) as described previously (Cheng et al., 2011). For HA immunostaining, neurons or HEK 293T cells were subjected to immunocytochemistry using HA antibody (Covance, Princeton, NJ, USA) according to the manufacturer's instructions. For myelin coating, polyornithine-coated glass coverslips were incubated with 40 μg/ml myelin (isolated from the brains of 3- to 6-month-old mice) in PBS overnight at 4°C. Cerebellar granule neurons were plated on either polyornithine- or polyornithine/myelin-coated glass coverslips and transfected 8 hours later as described above.

Axon growth assays

Axon growth assays were performed as described previously (Konishi et al., 2004; Stegmüller et al., 2006). Images of GFP-positive neurons were captured by a blinded observer using an Eclipse Ti epifluorescence microscope (Nikon, Tokyo, Japan). Axon growth was analyzed by measuring axon lengths using ImageJ software (NIH). GraphPad Prism software was used to perform statistical tests including ANOVA and unpaired *t*-tests.

Co-immunoprecipitation, subcellular fractionation, ubiquitylation assays and immunoblotting

For co-immunoprecipitation analyses, lysates of transfected 293T cells (exogenous) or P9 mouse cortex (endogenous) were prepared in buffer containing 1% NP40, 150 mM NaCl, 210 mM Tris pH 7.4, 1 mM EDTA, 10% glycerol (plus protease inhibitors). Lysates were incubated with c-Myc (Santa Cruz), HA (Covance), Cdh1 (Sigma), Flag (Sigma) or GFP (Invitrogen) antibody (0.8 μg of antibodies in 1 mg lysate) at 4°C for 4 hours in a tumbler and subsequently with Protein A-Sepharose beads (GE Healthcare) for 1 hour. The protein-bound beads were washed three times with Triton X-100 buffer (1 M NaCl, 50 mM Tris-HCl pH 7.5, 1 mM EDTA, 1% Triton X-100) and once with PBS. The bound protein was eluted by boiling the beads in SDS Laemelli buffer.

For subcellular fractionation, neurons in culture were scraped into detergent-free buffer A (10 mM HEPES pH 7.9, 10 mM KCl, 0.1 mM EDTA, 0.1 mM EGTA, protease inhibitors) and mechanically disrupted using a 2-ml dounce homogenizer. Nuclei were spun down at 500 ***g*** at 4°C and the supernatant was collected as the cytoplasmic fraction. Nuclei were subjected to one wash in 0.1% NP40-supplemented buffer A and then lysed in buffer B (20 mM HEPES pH 7.9, 400 mM NaCl, 1 mM EDTA, 1 mM EGTA, protease inhibitors) and pelleted at maximum speed (18,400 ***g***) at 4°C. The supernatant was collected as the nuclear fraction.

For cell-based ubiquitylation assays, lysates of transfected 293T cells were prepared in denatured modified RIPA buffer (50 mM Tris pH 7.5, 150 mM NaCl, 0.1% SDS, 0.5% sodium deoxycholate, 1% NP40, 10 mM N-ethylmaleimide, protease inhibitors) to rule out non-specific ubiquitylation detection, as described previously (Cui et al., 2011). Thereafter, the lysates were incubated with the HA antibody at 4°C for 2 hours and then with Protein A-Sepharose beads for 45 minutes. The protein-bound beads were washed three times with Triton X-100 buffer and once with PBS. The bound protein was eluted by boiling the beads in SDS Laemelli buffer.

SDS-PAGE and immunoblotting of lysates of tissues of rats at different embryonic and postnatal days and of granule neurons at different days in vitro were performed as previously described (Stegmüller et al., 2008). For ubiquitylation assays in *Cdh1* transgenic animals, total brain lysates of week-15 pups prepared in modified RIPA buffer were subjected to immunoprecipitation using the Smurf1 antibody and processed as described above.

RhoA pulldown assays

Cerebellar lysates of *Cdh1* transgenic animals prepared in 1% NP40, 150 mM NaCl, 210 mM Tris pH 7.4, 1 mM EDTA, 10% glycerol (plus protease inhibitors) were incubated with GST-Rhotekin-conjugated glutathione-Sepharose beads (GE Healthcare) at 4°C for 2 hours. Following three washes in lysis buffer, the bound RhoA-GTP was eluted by boiling in SDS Laemlli buffer and subjected to SDS-PAGE and western blotting.

Luciferase assays

293T cells transfected with Renilla-Smurf1 WT or Renilla-Smurf1 DBM3/4 expression plasmid were lysed using passive lysis buffer (Promega, Madison, WI, USA). The lysates were subjected to a Dual Luciferase Assay (Promega). SV40 firefly luciferase (pGL3 basic promoter) expression plasmid was co-expressed in all the experiments and firefly activity served as the internal reference.

Confocal imaging

For confocal imaging of RhoA/GFP at axonal tips, we used a Leica TCS SP2 confocal microscope with a 63× oil-immersion objective. To evaluate RhoA and GFP intensity, the mean gray values at corresponding regions of interest were determined using ImageJ software.

RESULTS

Cdh1-APC-mediated axon growth suppression is dependent on RhoA

To examine how Cdh1-APC inhibits axon growth and where this pathway interacts with myelin-mediated suppression of axon growth, we tested the hypothesis that the key downstream regulator of Nogo receptor signaling, RhoA, is important in Cdh1-APC-

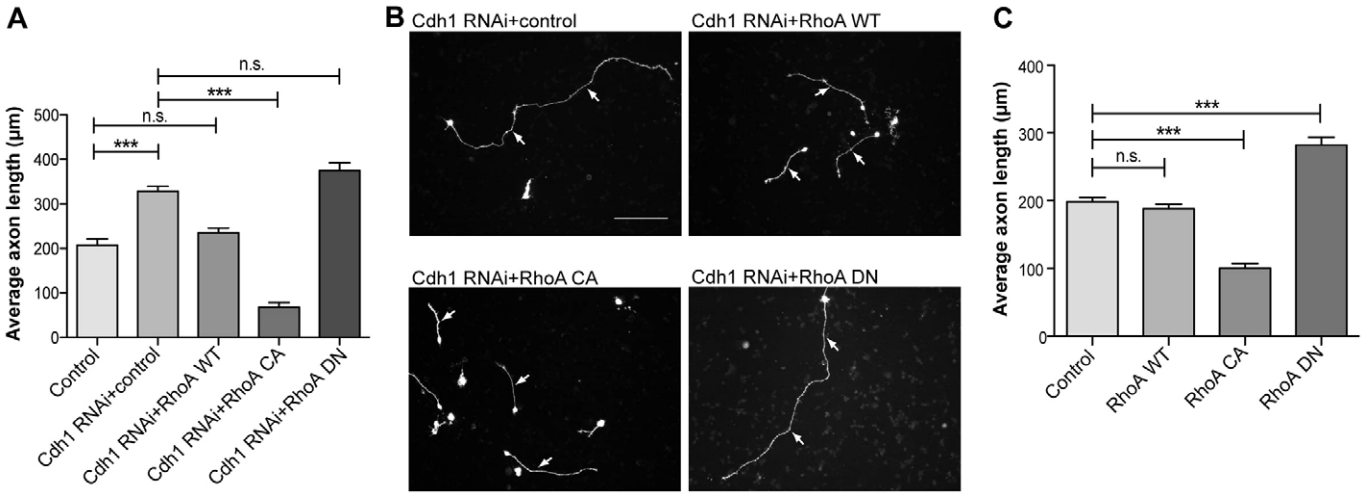

Fig. 1. Cdh1-APC-mediated axon growth suppression is dependent on RhoA. (**A**) Cerebellar granule neurons were transfected 8 hours after plating [day in vitro (DIV) 0] with the control vector U6 or the Cdh1 RNAi plasmid together with empty control vector pCEFL, the plasmid expressing wild-type (WT), constitutively active (CA) or dominant-negative (DN) RhoA. At DIV 3, neurons were subjected to immunocytochemistry using GFP antibody. Axonal length was measured in GFP-positive transfected neurons using ImageJ. A total of 443 neurons were measured. (**B**) Representative images of transfected neurons from A. Arrows indicate axons. Scale bar: 100 μm. (**C**) Granule neurons were transfected at DIV 0 with control vector or plasmids encoding RhoA WT, RhoA CA or RhoA DN together with the GFP plasmid. At DIV 3, neurons were analyzed as in A. A total of 717 neurons were measured. (A,C) ANOVA, ***P<0.0001; n.s., non-significant; mean + s.e.m.

mediated axon growth control (McGee and Strittmatter, 2003; Schwab, 2004). We determined in epistasis analyses whether the small Rho GTPase RhoA acts downstream of Cdh1-APC-mediated axon growth suppression. We triggered RNAi-induced knockdown of Cdh1 in cultured cerebellar granule neurons in which we simultaneously expressed plasmids that encode wild-type (WT) RhoA, or its constitutively active (CA) or dominant-negative (DN) forms (Coso et al., 1995). The DN and CA constructs of Rho GTPases have been extensively used in the past to study the effects of mutants that mimic the GDP- and GTP-bound states of Rho GTPases (Aoki et al., 2004; Kranenburg et al., 1997; Luo et al., 1994; Sarner et al., 2000; Schwamborn and Püschel, 2004). As previously reported, we found enhanced axon growth in Cdh1 knockdown neurons as compared with control neurons (Konishi et al., 2004). Co-expression of RhoA DN has little or no effect on Cdh1 knockdown-enhanced axonal length. By contrast, expression of RhoA WT decreases axon length and expression of RhoA CA results in an even more dramatic reduction of axonal length (Fig. 1A,B), suggesting that RhoA, and in particular active RhoA, counteracts the Cdh1 knockdown effect.

We also compared these results with the effects of the different forms of RhoA on axon growth without simultaneous Cdh1 knockdown and found that RhoA WT has little or no effect on axon growth, whereas RhoA CA inhibits and RhoA DN stimulates axon growth (Fig. 1C). The absence of an overt axon growth phenotype upon overexpression of RhoA WT suggests that there is a tight regulation of Rho GTPase activity by RhoA guanine nucleotide exchange factors (RhoGEFs) and RhoA GTPase activating proteins (RhoGAPs) and/or regulated protein turnover. This is however overcome when DN and CA mutants are expressed owing to their mimicking of constitutive GDP- or GTP-bound states. While acknowledging that RhoA is involved in many pathways of neurite growth regulation (Govek et al., 2005), our finding that RhoA counteracts Cdh1 knockdown-enhanced axon growth prompted us to postulate that RhoA is also a downstream component of the Cdh1-APC pathway.

Cdh1 interacts with the E3 ubiquitin ligase Smurf1

RhoA plays an essential role in axon growth control and is a crucial downstream component of myelin inhibition of axon growth (Domeniconi et al., 2005; Fournier et al., 2003; Govek et al., 2005; Hata et al., 2006; Wang et al., 2002; Winzeler et al., 2011; Wong et al., 2002). Given that Cdh1 knockdown overrides myelin inhibition of axon growth (Konishi et al., 2004), this raises the question of how Cdh1-APC might control RhoA. Since both Cdh1-APC and RhoA act as axon growth inhibitors, RhoA is unlikely to be a substrate of the E3 ligase Cdh1-APC. Hence, we reasoned that Cdh1-APC might control a substrate that in turn controls RhoA.

Aside from being regulated by specific GAPs and GEFs, RhoA has also been identified as a substrate of the E3 ubiquitin ligase Smurf1 (Wang et al., 2003). Smurf1 polyubiquitylates RhoA and targets it for proteasomal degradation (Wang et al., 2003). Thus, we asked whether Cdh1-APC might target Smurf1 for degradation to efficiently control RhoA activity. We first performed co-immunoprecipitation analyses in heterologous cells expressing exogenous Cdh1 and Smurf1 or Smurf2. We then immunoprecipitated Cdh1 and immunoblotted for Smurf1 or for the Smurf1 homolog Smurf2. We found that Cdh1 specifically interacts with Smurf1 but not with Smurf2 (Fig. 2A,B). In a reciprocal experiment we immunoprecipitated Smurf1 and immunoblotted for Cdh1. This experiment confirmed the Cdh1-Smurf1 interaction (Fig. 2C). To establish the endogenous association of Cdh1 and Smurf1 in the brain, we first confirmed that the Cdh1 polyclonal antibody, which was generated against a Cdh1 peptide, precipitates Cdh1 from brain lysates by co-immunoprecipitating Cdh1 together with the APC subunit Cdc27 (supplementary material Fig. S1). We then corroborated the interaction of Cdh1 and Smurf1 using brain lysates (Fig. 2D). These experiments identify the E3 ligase Smurf1 as a novel interactor of Cdh1.

Smurf1 is abundantly expressed in the brain

Smurf1 is abundantly expressed in the cerebellum, cortex and hippocampus (Fig. 3A), with levels decreasing with age in the

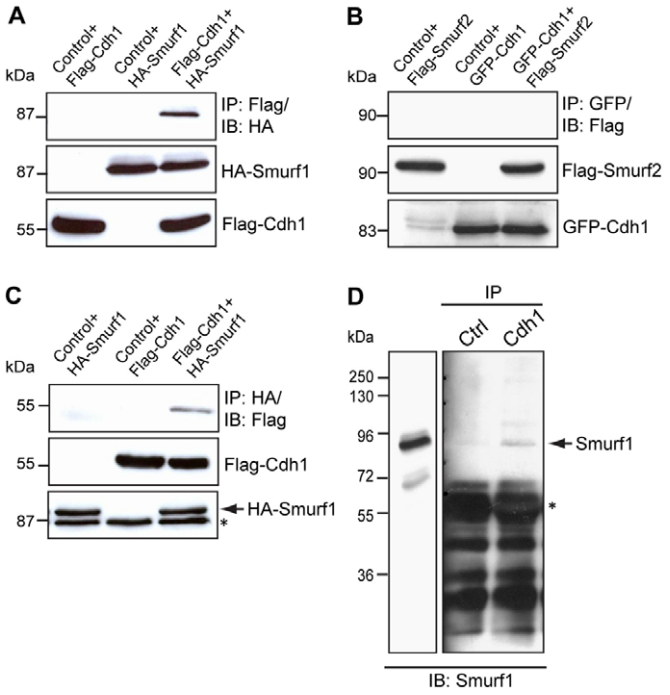

Fig. 2. Cdh1 interacts with the E3 ubiquitin ligase Smurf1. (**A**) Lysates of 293T cells transfected with empty vector pCMV5 and the Flag-Cdh1 and/or HA-Smurf1 expression plasmids were subjected to immunoprecipitation with Flag antibody and immunoblotted with HA antibody. (**B**) Lysates of 293T cells transfected with GFP and Flag-Smurf2 expression plasmids, GFP-Cdh1 plasmid and empty vector pCMV5 or both GFP-Cdh1 and Flag-Smurf2 plasmids were subjected to immunoprecipitation with GFP antibody and immunoblotted with Flag antibody. (**C**) Reciprocal co-immunoprecipitation to A. Asterisk indicates non-specific bands. (**D**) P9 mouse total brain lysates were immunoprecipitated with preimmune serum or Cdh1 antiserum followed by immunoblotting with Smurf1 antibody. Asterisk indicates IgG_H.

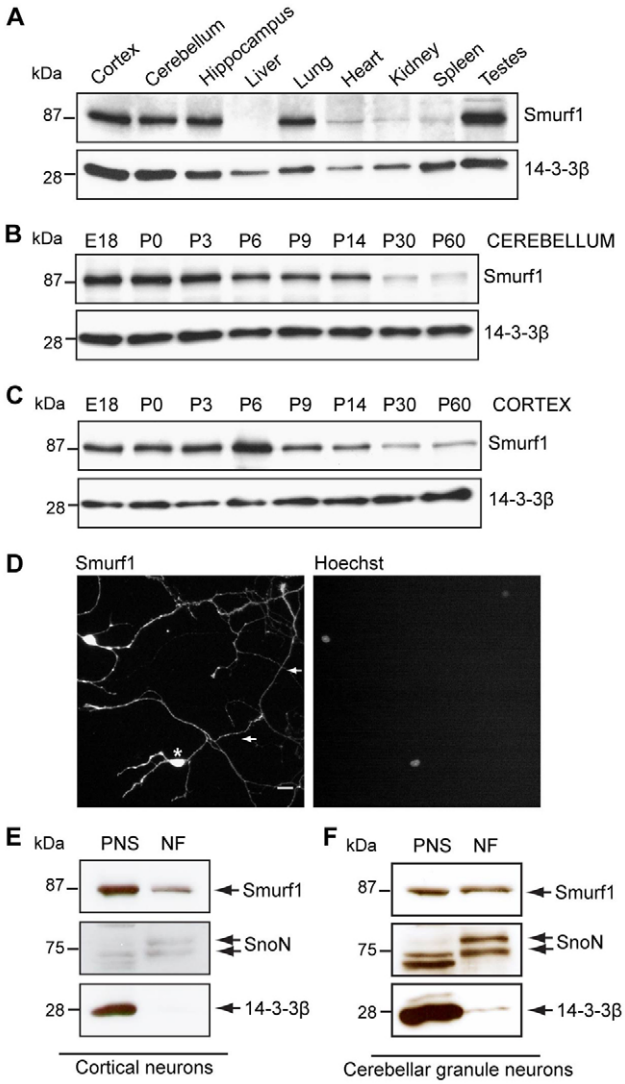

Fig. 3. Smurf1 expression in the brain and in neurons. (**A**) Lysates of the indicated tissues collected from wild-type P20 mouse were subjected to immunoblotting using Smurf1 antibody. 14-3-3β served as loading control. (**B**) Cerebella were collected from wild-type rats at the indicated days and lysates were subjected to immunoblotting using Smurf1 antibody. (**C**) Cortices were collected from wild-type rats at the indicated days and lysates were analyzed as described in A. (**D**) Cerebellar granule neurons at DIV2 were subjected to immunocytochemistry with Smurf1 antibody and staining with the nuclear dye bisbenzimide Hoechst 33258. Arrows and asterisk indicate axons and soma, respectively. Scale bar: 10 μm. (**E**) Cerebellar granule neurons were subjected to subcellular fractionation. Nuclear (NF) and postnuclear supernatant (PNS) fractions were immunoblotted using Smurf1, SnoN and 14-3-3β antibodies. SnoN and 14-3-3β served as controls for NF and PNS, respectively. (**F**) Cortical neurons were subjected to subcellular fractionation analyses as described in E.

cerebellum and cortex (Fig. 3B,C). At the subcellular level, Smurf1 is present in both the nuclear and cytoplasmic compartments of cultured granule neurons (Fig. 3D). These findings are supported by subcellular fractionation analysis demonstrating the nuclear and cytoplasmic localization of Smurf1 in both cerebellar granule neurons and cortical neurons (Fig. 3E,F).

Smurf1 is degraded by the proteasome and accumulates upon reduced Cdh1 levels in the brain

To determine whether Smurf1 is a substrate of Cdh1-APC, we first investigated if Smurf1 undergoes proteasome-dependent turnover in neurons. We treated granule neurons with the proteasome inhibitor lactacystin or vehicle and found that Smurf1 accumulates upon proteasome inhibition (Fig. 4A). We next determined the Cdh1-APC-dependent stability of Smurf1. For this, we made use of a *Cdh1* gene trap mouse line, which displays a reduced level of Cdh1 in heterozygous animals (Li et al., 2008). Owing to the early embryonic lethality of the *Cdh1* knockout, we performed our analyses on tissues collected from $Cdh1^{+/-}$ animals. We analyzed cerebella isolated from wild-type and $Cdh1^{+/-}$ mice at different ages and detected an accumulation of Smurf1 in the latter (Fig. 4B). To demonstrate that this change in Smurf1 protein level is not a result of enhanced transcription of the *Smurf1* gene, we carried out quantitative RT-PCR and detected no significant difference in mRNA levels in wild-type as compared with $Cdh1^{+/-}$ cerebella (Fig. 4C). In addition, we subjected the wild-type and $Cdh1^{+/-}$ brains to Smurf1 immunoprecipitation followed by immunoblotting with ubiquitin and found a slight but consistent decrease in Smurf1 ubiquitylation (Fig. 4D,E). These data suggest that Smurf1 is

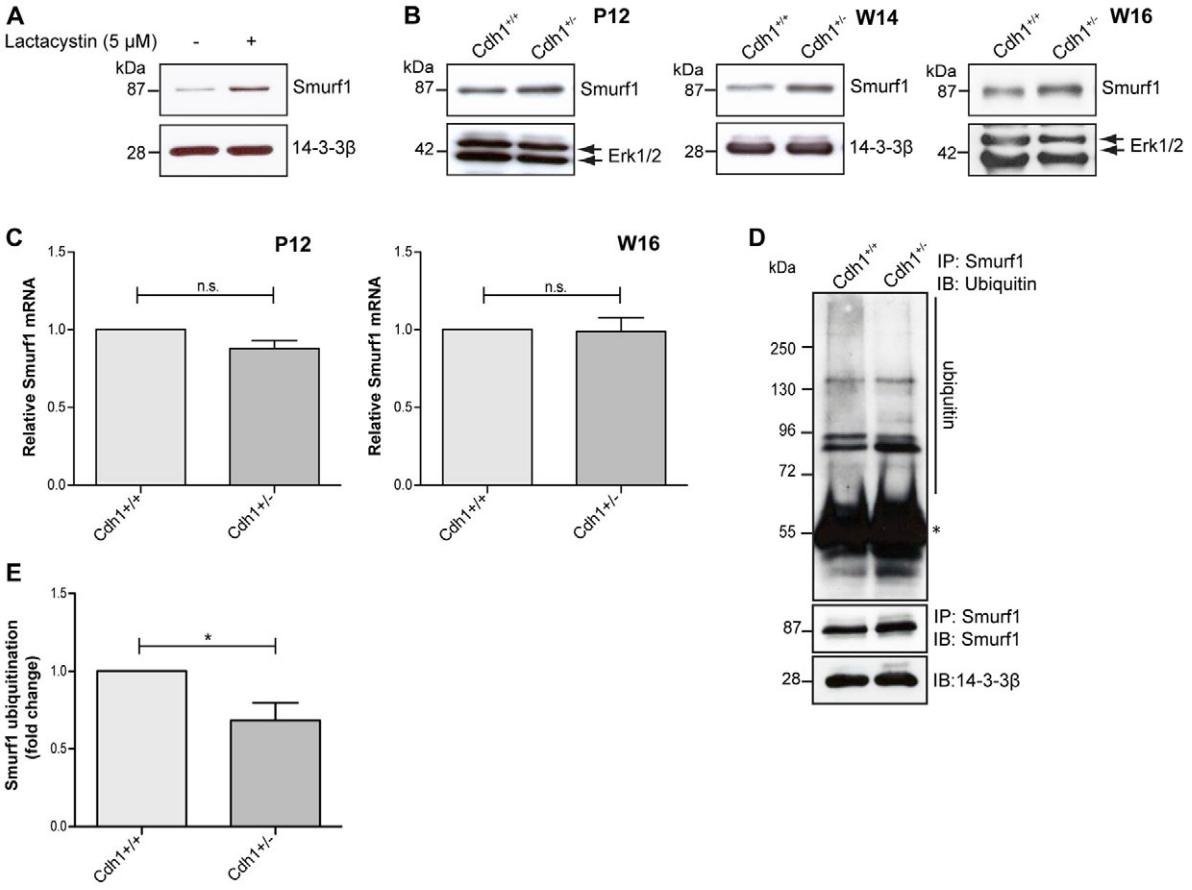

Fig. 4. Smurf1 is degraded in a proteasome- and Cdh1-APC-dependent manner. (**A**) Lysates of granule neurons treated with vehicle or 5 μM lactacystin for 9 hours were subjected to immunoblotting using Smurf1 antibody. 14-3-3β served as the loading control. (**B**) Cerebellar lysates of P12, week (W) 14 and W16 *Cdh1*$^{+/+}$ and *Cdh1*$^{+/-}$ mice were immunoblotted using Smurf1 antibody. 14-3-3β and Erk1/2 served as loading controls. (**C**) Total mRNA was isolated from cerebella of P12 and W16 *Cdh1*$^{+/+}$ and *Cdh1*$^{+/-}$ mice and subjected to quantitative RT-PCR using *Smurf1*-specific primers. *Smurf1* expression was normalized to *Gapdh* (P12) and β-actin (W16). n.s., non-significant (*t*-test, $P>0.05$); $n=8$ for P12 and $n=4$ for W16; mean + s.e.m. (**D**) Total brain lysates of W15 *Cdh1*$^{+/+}$ and *Cdh1*$^{+/-}$ mice were subjected to immunoprecipitation with Smurf1 antibody and immunoblotting using ubiquitin and Smurf1 antibodies. (**E**) The intensity of Smurf1 ubiquitylation was quantified and normalized to that of 14-3-3β using ImageJ. *t*-test; *$P<0.05$.

degraded by the 26S proteasome and that Smurf1 ubiquitylation and total protein levels depend on Cdh1-APC.

Smurf1 is a novel substrate of Cdh1-APC

Substrates of Cdh1 harbor signature recognition motifs including the destruction box (D-box), KEN box or A-box (Glotzer et al., 1991; Littlepage and Ruderman, 2002; Pfleger and Kirschner, 2000). We found several potential D-boxes in the Smurf1 amino acid sequence. Previous reports demonstrated that mutation of the D-box stabilizes the substrates as a result of reduced or abolished binding to Cdh1 (Lasorella et al., 2006; Stroschein et al., 2001). We carried out site-directed mutagenesis to individually mutate all five potential D-boxes of human *SMURF1*, of which only 3, 4 and 5 are conserved down to *Drosophila.* We then transfected neurons with plasmids encoding Smurf1 D-box mutant 1 (DBM1), Smurf1 DBM2, Smurf1 DBM3, Smurf1 DBM4, Smurf1 DBM5 and Smurf1 wild type (WT) as control and subjected these neurons to lactacystin treatment. We then analyzed the neuronal lysates and found that DBM1, DBM2 and DBM5, as well as Smurf1 WT, accumulate upon lactacystin treatment, whereas DBM3 and DBM4 fail to respond (Fig. 5A). These experiments suggest that DBM3 and DBM4 are putative D-boxes.

Next, we explored whether mutated D-boxes alter the binding affinity of Smurf1 for Cdh1 and found that all single mutants interact equally well with Cdh1 (supplementary material Fig. S2A). Thus, we generated a Smurf1 double mutant (Smurf1 DBM 3/4) and carried out co-immunoprecipitation experiments in which we immunoprecipitated Cdh1 and immunoblotted for Smurf1. We found that Smurf1 DBM3/4 binds to Cdh1 with a significantly weaker affinity than Smurf1 WT (Fig. 5B). In addition, Smurf1 DBM3/4 is considerably more stable than its wild-type counterpart (Fig. 5C). To quantify the stabilization of Smurf1 DBM3/4, we fused Renilla luciferase to Smurf1 or Smurf1 DBM 3/4 and carried out a dual luciferase assay. We found an increase in Renilla-Smurf1 DBM 3/4 activity as compared with Renilla-Smurf1 WT (Fig. 5D), which reflects the increase in protein stability shown in Fig. 5C. Notably, the importance of Smurf1 D-boxes 3 and 4 is supported by their conservation from fly to human (Fig. 5E). Also, we found that Smurf1 WT is ubiquitylated to a much higher extent than Smurf1 DBM3/4 (Fig. 5F). These data suggest that the Smurf1 double D-box mutant is markedly stabilized and that the Cdh1-Smurf1 interaction involves two D-box motifs.

To establish whether Smurf1 is a substrate of Cdh1-APC, we performed a cell-based assay to monitor the ubiquitylation of

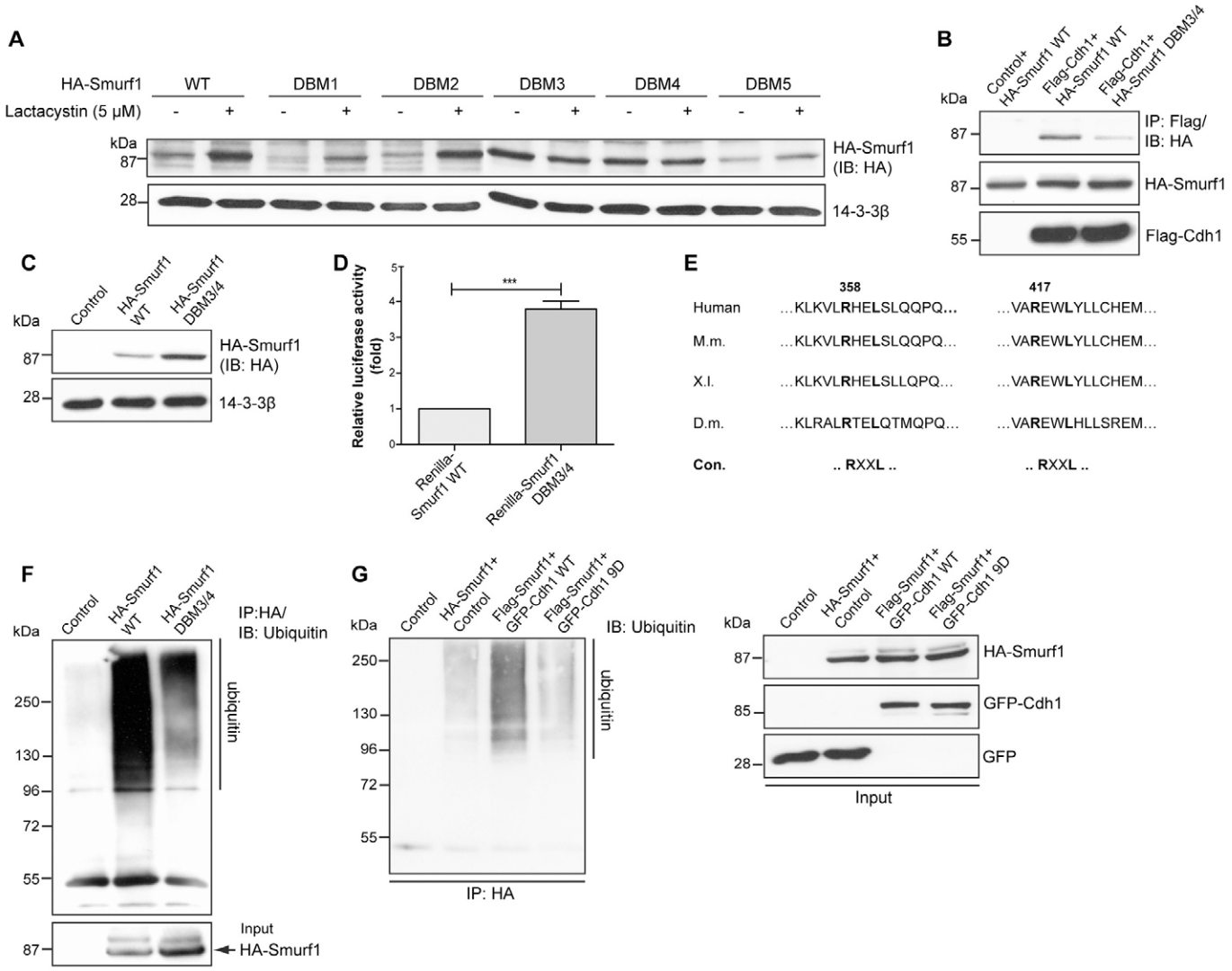

Fig. 5. Smurf1 is ubiquitylated and degraded in a destruction box-dependent manner by Cdh1-APC. (**A**) Granule neurons were transfected with HA-tagged Smurf1 WT or the five potential Smurf1 D-box mutants (DBM1-5) and treated with vehicle or 5 μM lactacystin. After 9 hours, lysates were collected and immunoblotted using HA antibody. 14-3-3β served as loading control. (**B**) Lysates of 293T cells transfected with a plasmid encoding HA-Smurf1 WT and empty vector pCMV5 or the Flag-Cdh1 plasmid or both HA-Smurf1 DBM3/4 and Flag-Cdh1 plasmids were subjected to immunoprecipitation using Flag antibody followed by immunoblotting with HA antibody. (**C**) Lysates of 293T cells transfected with equal amounts of HA-Smurf1 WT or HA-Smurf1 DBM3/4 plasmids were subjected to immunoblotting with HA antibody. (**D**) 293T cells transfected with Renilla-Smurf1 WT or Renilla-Smurf1 DBM3/4 expression plasmid together with the SV40 firefly luciferase (pGL3 promoter) plasmid (which serves as an internal control for transfection efficiency) were subjected to luciferase assay. *t*-test, ***P<0.0001; n=8; mean + s.e.m. (**E**) Smurf1 amino acid sequence showing conservation of D-boxes. M.m., *Mus musculus*; X.l., *Xenopus laevis*; D.m., *Drosophila melanogaster*; Con, consensus. (**F**) Lysates of 293T cells transfected with control vector pCMV5, HA-Smurf1 WT or HA-Smurf1 DBM3/4 plasmids were subjected to immunoprecipitation using HA antibody followed by immunoblotting using ubiquitin antibody. (**G**) Lysates of 293T cells transfected with control vector pCMV5 and pEGFP or Smurf1 plasmid together with pEGFP, Cdh1 WT or Cdh1 9D expression plasmid were subjected to immunoprecipitation with HA antibody followed by immunoblotting with ubiquitin antibody.

Smurf1 by Cdh1-APC. We immunoprecipitated exogenous Smurf1 from heterologous cells in control, Cdh1 wild-type (WT) or Cdh1 9D overexpression conditions and immunoblotted the precipitates with a ubiquitin antibody. Cdh1 9D is a hyperphosphomimetic, loss-of-function mutant that does not bind to the APC core (Huynh et al., 2009) but binds to Smurf1 (supplementary material Fig. S2B). Although Smurf1 is ubiquitylated in control conditions, expression of Cdh1 stimulates the extent of Smurf1 ubiquitylation, whereas Cdh1 9D fails to trigger this effect (Fig. 5G). These experiments suggest a specific Cdh1-APC-mediated ubiquitylation and degradation of Smurf1.

Smurf1 promotes axon growth

Smurf1 has previously been implicated in neurite growth in neuroblastoma cells (Bryan et al., 2005) and in axon initiation and growth in neurons (Cheng et al., 2011; Sato and Heuckeroth, 2008). We asked whether Smurf1 regulates axonal growth in a Cdh1-APC/Smurf1 axis. We first generated a Smurf1 RNAi plasmid based on a targeting region identified by Boyer and colleagues (Boyer et al., 2006) and validated the efficient knockdown in heterologous cells (Fig. 6A). In addition, we found loss of endogenous Smurf1 in 74% of Smurf1 RNAi-transfected neurons, whereas all control-transfected neurons

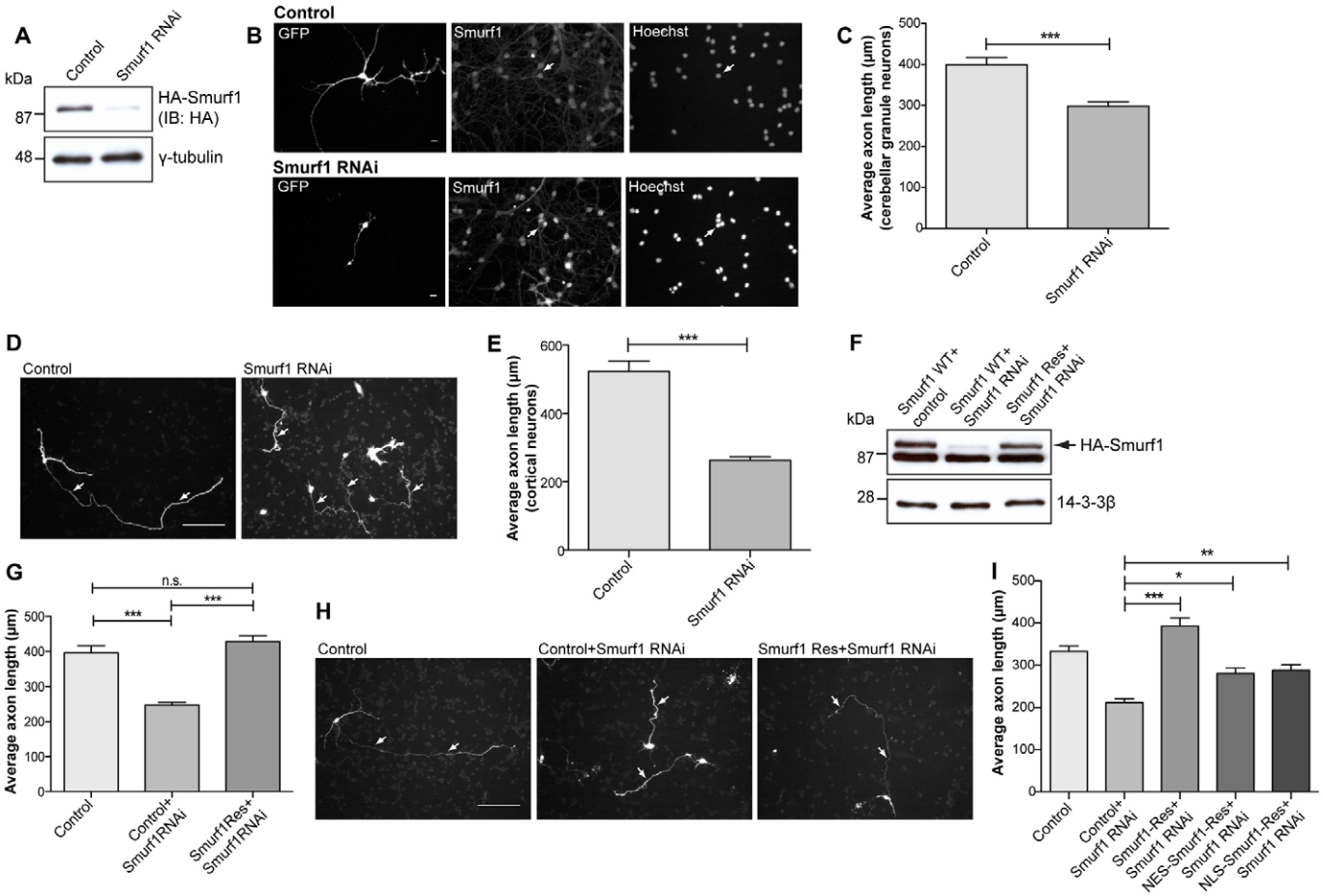

Fig. 6. Smurf1 promotes axon growth. (**A**) 293T cells were transfected with a plasmid encoding HA-Smurf1 together with control vector U6 or the Smurf1 RNAi plasmid. Lysates were subjected to immunoblotting using HA antibody. γ-tubulin served as the loading control. (**B**) Granule neurons were transfected with control vector U6 or the Smurf1 RNAi plasmid together with a plasmid encoding farnesylated GFP and subjected to immunocytochemistry with Smurf1 and GFP antibodies. Arrows indicate control transfected Smurf1-positive neurons and Smurf1 knockdown neurons. (**C**) Cerebellar granule neurons were transfected at DIV 0 with the control vector U6 or Smurf1 RNAi plasmid. At DIV 4, neurons were analyzed as in Fig. 1A. A total of 384 neurons were measured. (**D**) Representative images of transfected neurons in C. Arrows indicate axons. (**E**) Cortical neurons were transfected at DIV 1 with the control vector U6 or Smurf1 RNAi plasmid. At DIV3, neurons were analyzed as in Fig. 1A. A total of 292 neurons were measured. (**F**) Lysates of 293T cells transfected with HA-tagged Smurf1 WT plasmid and the empty vector U6, Smurf1 RNAi plasmid and empty vector pCMV5 or the Smurf1 rescue (Smurf1 Res) plasmid were immunoblotted using HA antibody. 14-3-3β served as loading control. (**G**) Cerebellar granule neurons were transfected at DIV 0 with control vector pCMV5 and U6, Smurf1 RNAi plasmid and the empty vector pCMV5 or the Smurf1-Res plasmid. At DIV4, neurons were analyzed as in Fig. 1A. A total of 425 neurons were measured. (**H**) Representative images of transfected neurons in G. Arrows indicate axons. (**I**) Granule neurons transfected with control vectors U6 and pCMV5, Smurf1 RNAi and pCMV5 plasmid, or Smurf1 RNAi plasmid together with the Smurf1-Res, NES-Smurf1-Res or the NLS-Smurf1-Res expression plasmid were analyzed at DIV4 as described in Fig. 1A. A total of 1076 neurons were measured. ANOVA (G,I) or *t*-test (C,E), ***P<0.0001, **P<0.001, *P<0.05; n.s., non-significant; mean + s.e.m. Scale bars: 10 μm in B; 100 μm in D,H.

were Smurf1 positive. These experiments thus established efficient knockdown of Smurf1 (Fig. 6B).

We then examined whether Smurf1 regulates axon growth in cerebellar granule neurons, which were transfected with control vector or the Smurf1 RNAi plasmid. Knockdown of Smurf1 led to a significant decrease in axonal length (Fig. 6C,D). We also found that Smurf1 knockdown reduces axonal length in cortical neurons (Fig. 6E). To ensure that the Smurf1 RNAi phenotype is specific and to rule out off-target effects, we constructed a Smurf1 RNAi-resistant form of Smurf1 (Smurf1-Rescue, or Smurf1-Res) by introducing four silent mutations into the RNAi targeting region in Smurf1 WT, and validated the Smurf1-Res-encoding plasmid in heterologous cells (Fig. 6F). Whereas Smurf1 RNAi reduces Smurf1 WT, it fails to knock down Smurf1-Res. In axon growth assays using granule neurons, we analyzed control neurons, Smurf1 knockdown neurons and Smurf1 knockdown neurons that express Smurf1-Res, and found that Smurf1-Res restores axonal length (Fig. 6G,H), thus indicating a specific Smurf1 RNAi phenotype. These experiments demonstrate that Smurf1 promotes axon growth independently of the neuronal cell type.

To examine whether the nuclear or the cytoplasmic localization of Smurf1 is required for its function in axon growth, we generated Smurf1-Res mutants that harbor either a nuclear localization sequence (NLS) or a nuclear exclusion sequence (NES) and performed a rescue experiment. We confirmed the intended subcellular localization of NES-Smurf1-Res and NLS-Smurf1-Res in both heterologous cells and in

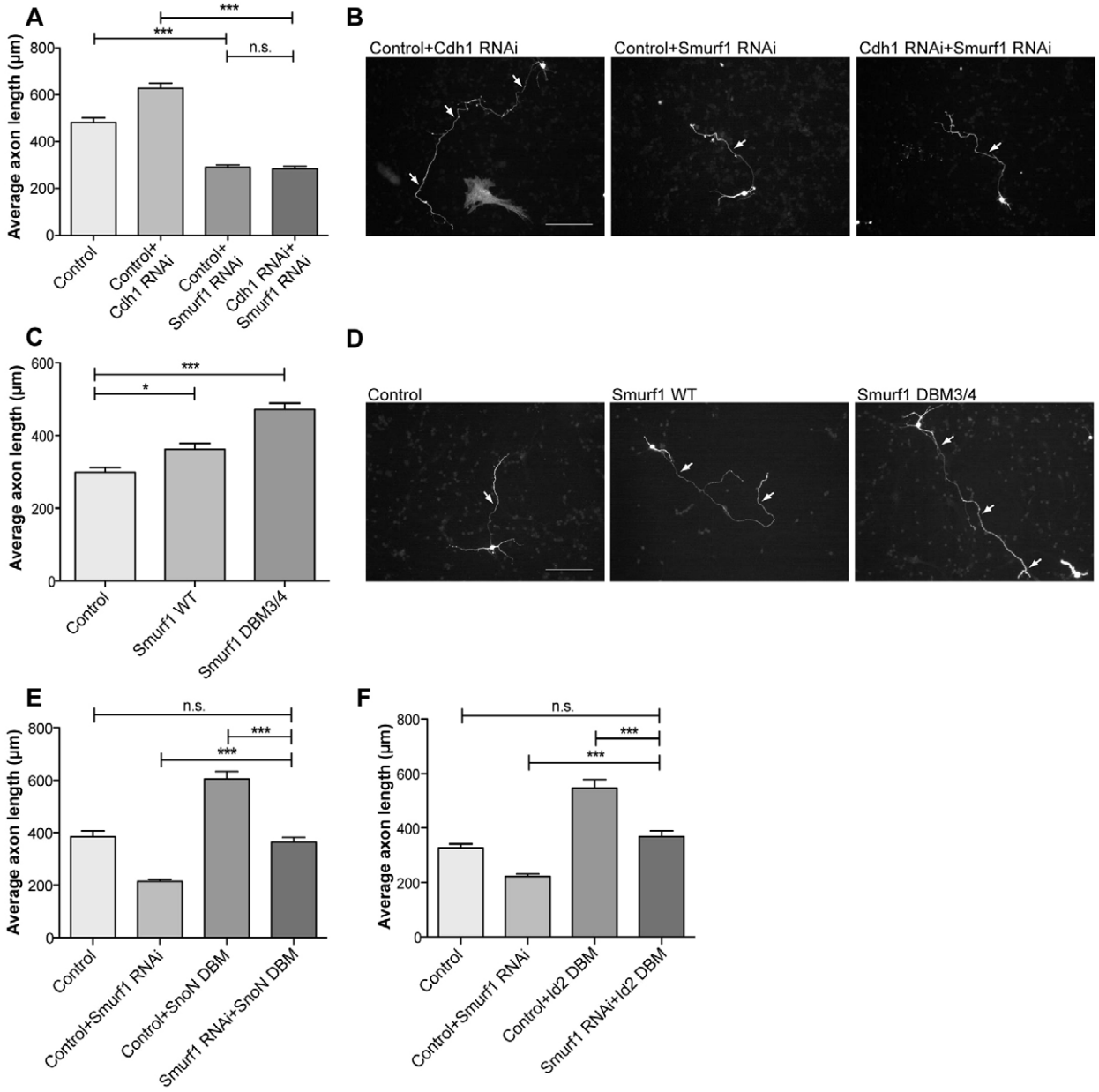

Fig. 7. Smurf1 acts downstream of Cdh1-APC but not SnoN or Id2 in axon growth. (**A**) Neurons transfected with control U6, U6 and Cdh1 RNAi, or U6 and Smurf1 RNAi or both Cdh1 RNAi and Smurf1 RNAi plasmids were analyzed at DIV4 as described in Fig. 1A. A total of 666 neurons were measured. (**B**) Representative images of transfected neurons in A. Arrows indicate axons. (**C**) Neurons were transfected with control vector pCMV5, Smurf1 WT or Smurf1 DBM3/4 expression plasmid together with GFP plasmid and analyzed at DIV 3 as in Fig. 1A. A total of 617 neurons were measured. (**D**) Representative images of transfected neurons in C. Arrows indicate axons. (**E**) Neurons transfected with control pCMV5 and U6 or Smurf1 RNAi, U6 and SnoN DBM, or both SnoN DBM and Smurf1 RNAi plasmids were analyzed at DIV4 as described in Fig. 1A. A total of 510 neurons were measured. (**F**) Neurons transfected with control pCDNA3 and U6 or Smurf1 RNAi, U6 and Id2 DBM, or both Id2 DBM and Smurf1 RNAi plasmids were analyzed at DIV4 as described in Fig. 1A. A total of 493 neurons were measured. (A,C,E,F) ANOVA, ***P<0.0001, *P<0.05; n.s., non-significant; mean + s.e.m. Scale bars: 100 μm.

neurons (supplementary material Fig. S3A,B). Whereas we found complete rescue of the Smurf1 phenotype by Smurf1-Res, expression of NLS-Smurf1-Res or NES-Smurf11-Res resulted in partial rescue, with significantly longer axons than Smurf1 RNAi neurons but significantly shorter axons than Smurf1 RNAi/Smurf1-Res neurons (Fig. 6I). These results suggest that Smurf1 is required both in the nucleus and in the cytoplasm to promote axon growth.

Smurf1 acts downstream of Cdh1-APC in axon growth but independently of SnoN or Id2

Having identified Smurf1 as a novel substrate of Cdh1-APC, we reasoned that Smurf1 might promote axon growth downstream of Cdh1-APC. In epistasis analyses, we addressed whether the Smurf1 RNAi phenotype overrules the Cdh1 RNAi phenotype to reveal that Smurf1 acts downstream of Cdh1 in axon growth control. In this experiment, we determined axon length of control neurons,

Cdh1 knockdown neurons, Smurf1 knockdown neurons, and neurons in which we triggered both Cdh1 and Smurf1 knockdown. Whereas Cdh1 knockdown stimulates and Smurf1 RNAi inhibits axon growth, knockdown of both Cdh1 and Smurf1 results in short axons (Fig. 7A,B). Since the dominant phenotype is triggered by Smurf1 knockdown, these data suggest that Smurf1 acts downstream of Cdh1 to regulate axon growth.

We then examined whether overexpression of Smurf1 induces the opposite effect on axon growth to Smurf1 RNAi. As the double D-box mutation of Smurf1 is substantially stabilized in neurons as compared with Smurf1 WT, we tested Smurf1 WT and Smurf1 DBM3/4 in gain-of-function analyses. We found that whereas Smurf1 WT has a moderate effect on axon growth, Smurf1 DBM3/4 leads to a considerable enhancement of axonal length (Fig. 7C,D), indicating that, as a consequence of stabilization, Smurf1 potently stimulates axonal growth.

Cdh1-APC controls several substrates in cell cycle regulation (Harper et al., 2002; Peters, 2002) and thus it is not surprising that, in order to regulate axon growth, Cdh1 targets more than the previously identified substrates SnoN and Id2 (Lasorella et al., 2006; Stegmüller et al., 2006) for degradation. To gain insight into the functional relationship of these substrates in axon growth regulation, we tested whether Smurf1 acts in either the SnoN or Id2 pathway and carried out further epistasis analyses. Since the Cdh1-degradation resistant D-box mutants of SnoN and Id2 promote axon growth (Lasorella et al., 2006; Stegmüller et al., 2006), we expressed SnoN DBM and Id2 DBM alone or together with Smurf1 RNAi plasmids and determined the dominant phenotype. For example, if Smurf1 were a downstream component of the SnoN or Id2 pathways, we would expect the Smurf1 RNAi phenotype to overrule the growth-promoting effect of SnoN or Id2. We found that whereas SnoN DBM and Id2 DBM promote axon growth and Smurf1 RNAi inhibits it, the axonal length of Smurf1 RNAi/SnoN DBM or Smurf1 RNAi/Id2 DBM neurons is significantly longer than that of Smurf1 RNAi axons but significantly shorter than that of SnoN DBM and Id2 DBM axons (Fig. 7E,F). These results indicate that Smurf1 is likely to control axon growth in a parallel pathway to SnoN and Id2.

Smurf1 controls axon growth and migration in vivo

To explore the role of Smurf1 in axonal development in the cerebellar cortex in vivo, we applied the in vivo electroporation technique to determine the effect of acute loss-of-function of Smurf1 (Konishi et al., 2004; Stegmüller et al., 2006). We injected bicistronic plasmids encoding Smurf1-targeting hairpins and an EGFP expression cassette, which were validated for efficient knockdown (Fig. 8A), into the cerebellum of P4 rat pups and subjected the animals to repeated electric pulses. Five days later, we analyzed coronal sections of control and knockdown animals. In control animals, the GFP-positive granule neurons descend into the internal granule layer, form bifurcated axons and develop a dendritic arbor. By contrast, knockdown of Smurf1 resulted in an overt phenotype, in which granule neurons stall in the external granular layer/molecular layer. When we quantified the migration defect, we found that whereas more than 90% of control neurons migrate into the internal granule layer, only 49% of Smurf1 knockdown neurons descend (Fig. 8B,C). Interestingly, immunohistochemical analysis in the P9 cerebellum revealed that Smurf1 is upregulated in neurons migrating through the molecular layer (supplementary material Fig. S4) and that Smurf1 knockdown neurons are stalled precisely at the border of the external granule layer and molecular layer (supplementary material Fig. S5A,B). These results suggest the requirement of Smurf1 for successful migration.

In addition to the migration defect, we found that the stalled neurons extend shorter and rather thick axons, which do not appear to develop into the characteristic parallel fibers of the control cerebellum (Fig. 8C, upper panel). Quantification of thick and thin processes demonstrated a clear defect in the Smurf1 knockdown cerebella, suggesting that Smurf1 is required for the proper development of parallel fibers (Fig. 8D,E). Furthermore, we determined the axon length of the transfected neurons. Since it is impossible to measure the parallel fibers of the control neurons, we measured the length of the parallel fibers as long as we could trace them in a section and thus determined the minimal length of these processes. In the knockdown condition, however, it was feasible to measure axonal length as we could determine the tips of the short axons. The measurements revealed that control axons extend for at least 390 μm, whereas knockdown of Smurf1 results in an average length of less than 120 μm (Fig. 8F).

Taken together, the in vivo analyses demonstrate that Smurf1 promotes proper neuronal migration and axon elongation in the developing cerebellar cortex.

Mediators of the Nogo pathway in Cdh1-APC/Smurf1-regulated axon growth

Having established the role of Smurf1 in axon growth, we went back to further examine RhoA as a key element in the Cdh1-APC/Smurf1 pathway of axon growth. To establish that Smurf1 DBM3/4-enhanced axon growth is indeed facilitated by RhoA, we examined whether Smurf1 DBM3/4 promotes axon growth in the presence of the Smurf1 degradation-resistant form of RhoA (RhoA K6,7R) (Ozdamar et al., 2005). We found that co-expression of RhoA WT, which is sensitive to Smurf1-mediated ubiquitylation and degradation, together with Smurf1 DBM3/4 has a reversing effect on axon growth as compared with Smurf1 DBM3/4 alone. However, co-expression of RhoA K6,7R counteracts the axon growth-stimulating phenotype of Smurf1 DBM3/4 in a more pronounced way (Fig. 9A,B). As a control, we co-expressed the small GTPase Cdc42 and found no effect on Smurf1 DBM3/4-stimulated axon growth (supplementary material Fig. S6). This result suggests that RhoA is an important downstream substrate of Smurf1 in axon growth. This finding, together with our immunocytochemical analyses showing that active RhoA is localized in the cytoplasm of neurons (supplementary material Fig. S7) and previous studies that have shown that Smurf1 regulates RhoA at the tips of processes in heterologous cells and in neurons (Cheng et al., 2011; Wang et al., 2003), indicate that RhoA turnover mediated by Smurf1 is an important cytoplasmic event in axon growth regulation.

To establish that the turnover of RhoA by Smurf1 contributes to Cdh1-mediated axon growth, we carried out axon growth assays in which we triggered Cdh1 knockdown and examined whether the Smurf1 degradation-resistant RhoA mutant dampens axon growth stimulation. We found that although the Cdh1 knockdown phenotype was significantly reduced in the presence of RhoA WT, this effect was even further enhanced in the presence of RhoA K6,7R (Fig. 9B). To examine whether RhoA levels are changed upon reduced Cdh1, we performed immunoblotting and RhoA activity assays in wild-type and *Cdh1* transgenic brains and found no difference in global RhoA levels or activity (supplementary material Fig. S8). We then determined by immunocytochemistry

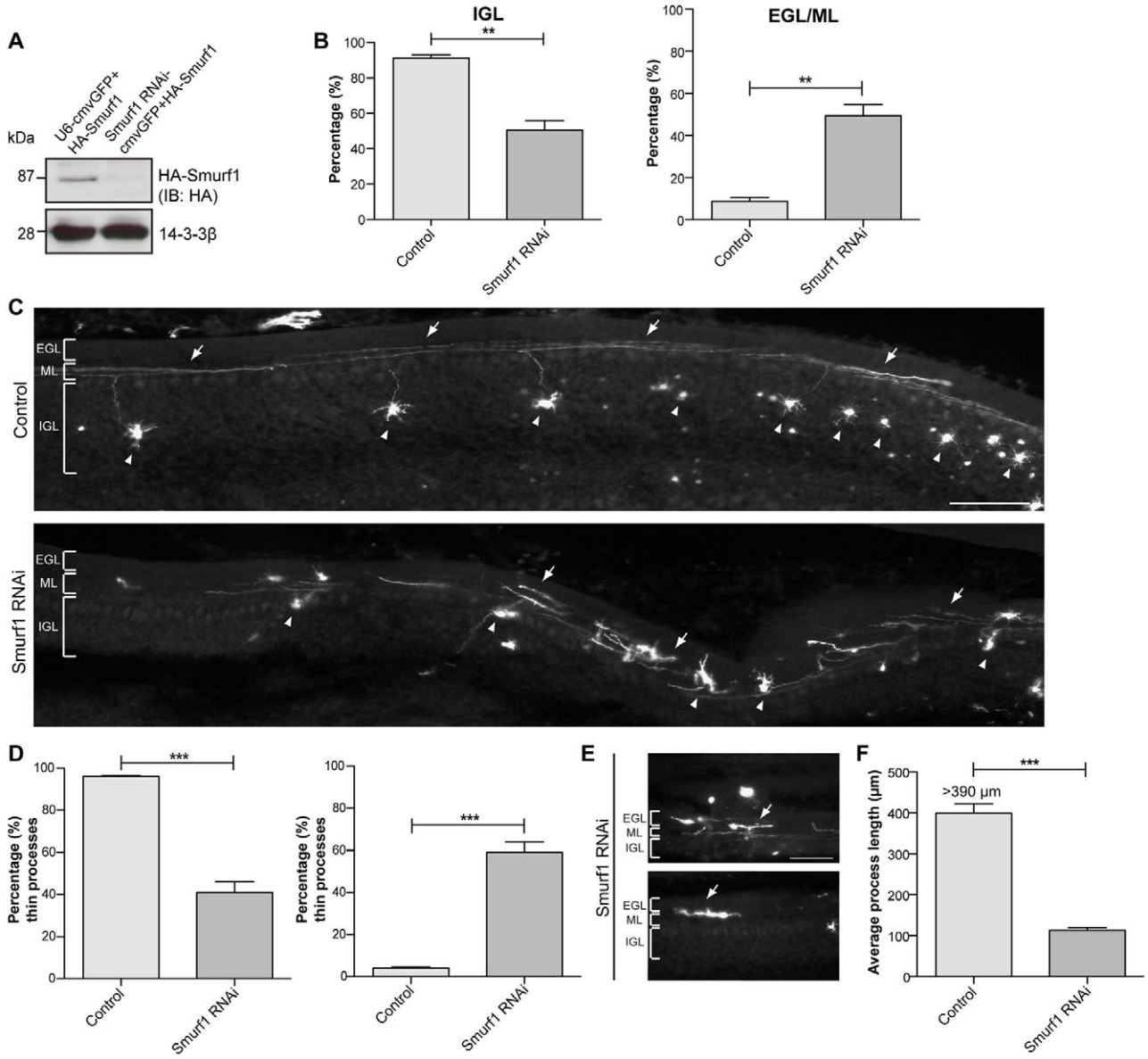

Fig. 8. Smurf1 promotes neuronal migration and axon elongation in the developing cerebellar cortex. (**A**) Lysates of 293T cells transfected with the control vector U6-CMV-EGFP or U6-Smurf1-CMV-EGFP together with the HA-Smurf1 expression plasmid were subjected to immunoblotting with HA and 14-3-3β (loading control) antibodies. (**B**) The control U6-CMV-EGFP plasmid or U6-Smurf1-CMV-EGFP plasmids were injected into the cerebellum of P4 rat pups. At P9, cerebella were isolated and coronal sections were subjected to immunohistochemistry using GFP antibody. The location of transfected neurons was assessed as either external granule layer/molecular layer (EGL/ML) or internal granule layer (IGL). A total of 10,527 neurons were counted. (**C**) Representative images of each condition in B. Arrows indicate parallel fibers and processes and arrowheads indicate cell bodies. (**D**) Quantification of thin (normal) processes and short thick processes. A total of 1200 processes were counted. (**E**) Representative images of Smurf1 knockdown neurons in vivo. Arrows indicate thick processes. (**F**) Quantification of process length. A total of 325 neurons were measured. ANOVA (D,F) or *t*-test (B), ***P<0.0001, **P<0.01; mean ± s.e.m. Scale bars: 100 μm.

whether RhoA levels are altered locally at the axonal tips and found robust downregulation in Cdh1 knockdown versus control neurons (supplementary material Fig. S9). These data strongly support the notion that the Cdh1-APC/Smurf1 pathway of axon growth inhibition regulates RhoA locally.

To underscore our initial finding that Cdh1-APC can modulate the response of axons to myelin inhibition, we determined whether Smurf1 is a crucial component in this process. In previous studies we have shown that Cdh1 knockdown overrules axon growth inhibition by myelin (Konishi et al., 2004). To examine the role of Smurf1 in this context, we measured axon lengths of control-transfected neurons on either a permissive adhesion substrate (polyornithine) or on myelin and compared them to Smurf1 DBM-expressing neurons on myelin. As expected, we found that myelin efficiently reduces axonal length as compared with neurons cultured on polyornithine. However, Smurf1 DBM-stimulated axon growth overcomes myelin inhibition and leads to significantly longer axons compared with control neurons on myelin (Fig. 9C,D). These experiments suggest that Smurf1 controls the responsiveness of axons to myelin.

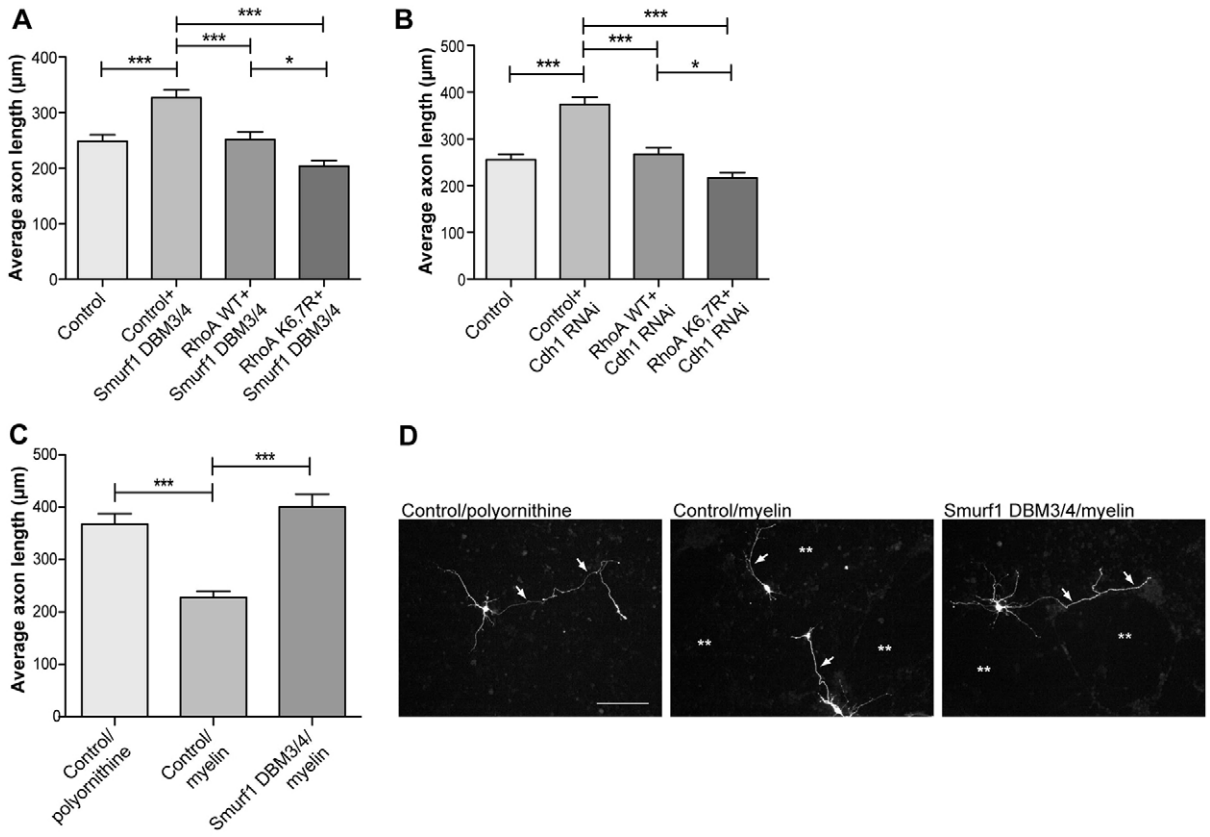

Fig. 9. Regulators of the Nogo pathway in Smurf1-mediated axon growth. (**A**) Neurons were transfected with control vectors pCMV5 and pCEFL, Smurf1 DBM3/4 expression plasmid together with pCEFL or plasmids encoding RhoA WT or RhoA K6,7R and analyzed at DIV 3 as in Fig. 1A. A total of 605 neurons were measured. (**B**) Neurons were transfected with control vectors U6 and pCEFL, Cdh1 RNAi plasmid together with pCEFL or plasmids encoding RhoA WT or RhoA K6,7R and analyzed at DIV 3 as in Fig. 1A. A total of 646 neurons were measured. (**C**) Cerebellar granule neurons cultured on polyornithine or polyornithine plus myelin (referred to as myelin) were transfected at DIV 0 with control pCMV5 or Smurf1 DBM3/4 plasmids and analyzed at DIV 4 as in Fig. 1A. A total of 414 neurons were measured. (A-C) ANOVA, ***P<0.0001, *P<0.05; mean + s.e.m. (**D**) Representative images of transfected neurons in C. Arrows indicate axons and asterisks indicate myelin-rich regions. Scale bar: 100 μm.

DISCUSSION

In this study, we delineated a mechanism by which Cdh1-APC-mediated axon growth suppression is supported by the RhoA-regulating E3 ubiquitin ligase Smurf1 (supplementary material Fig. S10). We identified Smurf1 as a novel substrate of Cdh1-APC and found that it is targeted in a D-box-dependent manner for proteasomal degradation. Our data indicate that Smurf1 acts downstream of Cdh1-APC but in parallel to the SnoN or Id2 pathway of axon growth control. We also found that acute knockdown of Smurf1 in vivo disrupts neuronal migration and axon growth in the developing cerebellar cortex. Finally, we found that the stabilized version of Smurf1 overcomes myelin-induced axon growth inhibition.

Our finding that the small GTPase RhoA plays a role in the Cdh1-APC pathway of axon growth regulation led us to discover the physical and functional association of Cdh1 with the RhoA-regulating E3 ligase Smurf1. Wang and colleagues have previously identified that Smurf1 targets RhoA for proteasome-dependent degradation (Wang et al., 2003). A recent study also reported the local degradation of RhoA in the tips of neuronal processes by Smurf1 during axon initiation (Cheng et al., 2011). These findings are consistent with our epistasis experiments, in which a Smurf1 degradation-resistant form of RhoA negates the growth-promoting effects of stabilized Smurf1 (Smurf1 DBM3/4) and Cdh1 knockdown, and with the finding that Cdh1 regulates RhoA levels locally at the axonal tips. In addition, our data together with recent reports establish that Smurf1 governs a generalizable mechanism of axon growth (Cheng et al., 2011; Vohra et al., 2007).

Smurf1 and Cdh1-APC are present in both the nucleus and cytoplasm (Stegmüller et al., 2006). We found that both the nuclear and cytoplasmic localization of Smurf1 contribute to axon growth. Previous studies found that Cdh1-APC appears to act solely in the nucleus to control axon growth and thus identified the transcriptional regulators SnoN and Id2 as substrates of Cdh1-APC in the control of axon growth (Lasorella et al., 2006; Stegmüller et al., 2006). With Smurf1, we found another nuclear target that underscores the importance of the nuclear activity of Cdh1-APC. However, our data also indicate that cytoplasmic Smurf1 controls axon growth. Owing to the predominant nuclear localization of Cdh1 (Konishi et al., 2004; Stegmüller et al., 2006) and its lower abundance and suggested localized activity in the cytoplasm, cytoplasmic Cdh1-APC might contribute to axon growth to a lesser extent than its nuclear activity. Also, our findings indicate that Smurf1 acts downstream of Cdh1-APC but do not support the notion that Smurf1 acts downstream of either SnoN or Id2.

With Smurf1 we identified the third substrate of Cdh1-APC in axon growth control and thus demonstrate that Cdh1-APC acts via multiple targets, a well-known concept from cell cycle

regulation by Cdh1-APC (Harper et al., 2002; Peters, 2002). The nuclear substrates of Cdh1-APC, SnoN and Id2, are degraded in a D-box-dependent manner and display a gain-of-function phenotype as the respective degradation-resistant D-box mutants promote axon growth (Lasorella et al., 2006; Stegmüller et al., 2006). Similar to SnoN and Id2, we identified D-box motifs in Smurf1 and found that a Smurf1 double D-box mutant stimulates axon growth. Also, our results indicate that, owing to reduced binding affinity to Cdh1, Smurf1 DBM3/4 is less ubiquitylated than Smurf1 WT and, consequently, is markedly stabilized. Collectively, these findings support the view that Smurf1 is a bona fide substrate of Cdh1-APC. A recent study that reports the interaction of Cdh1 and Smurf1 in osteoblasts suggests, in contrast to our findings, a non-proteolytic Cdh1 activity that promotes the autoubiquitylation of Smurf1 (Wan et al., 2011). It is very likely that the two mechanisms co-exist and that the preferred usage might be dependent on cell type.

Despite the abundance of Smurf1 in nervous tissue, deficiencies of the brain in the *Smurf1* knockout animal were not reported. The most overt phenotype of the *Smurf1* knockout mouse is an increase in bone mass (Yamashita et al., 2005). In *Xenopus*, however, disruption of Smurf1 expression leads to defects in neural development (Alexandrova and Thomsen, 2006). Recently, Cheng and colleagues found axon specification defects in in-vivo analyses of Smurf1 knockdown in the rodent cortex (Cheng et al., 2011). Our in vivo analyses demonstrate that acute knockdown of Smurf1 leads to a severe defect in axon growth and, in addition, to an impairment of granule neuron migration in the developing cerebellum, which underscores the role of Smurf1 in the developing mammalian brain and the importance of the tight regulation of RhoA by the Cdh1-APC/Smurf1 pathway. Cdh1 knockdown has previously been shown to result in a patterning defect characterized by axonal defasciculation in the cerebellar cortex (Konishi et al., 2004). A gain-of-function analysis of Cdh1 in the cerebellum has not been carried out owing to no gain of function of Cdh1 in axon grwoth (J.S. and A. Bonni, unpublished). A recent report suggests that the Cdh1 substrate SnoN controls the proper migration and positioning of neurons in the internal granule layer of the cerebellum (Huynh et al., 2011), indicating that Cdh1-APC governs several possibly interconnected mechanisms of neural development. Also, like the transcriptional regulator SnoN, Smurf1 is a component of the TGFβ/BMP signaling pathway in axon growth regulation. Previous studies have demonstrated that TGFβ signaling regulates Cdh1-APC/SnoN-mediated axon growth through Smad2 (Stegmüller et al., 2008).

The finding that Cdh1-APC controls the RhoA regulator Smurf1 might explain why enhanced axon growth due to Cdh1 knockdown, as well as that due to Smurf1 DBM3/4, overrules myelin inhibition, a process mediated by RhoA (Fournier et al., 2003; Giger et al., 2010; Konishi et al., 2004; McGee and Strittmatter, 2003; Schwab, 2004). That the Cdh1-APC pathway of axon growth suppression does play an essential role in the failure of CNS regeneration has been demonstrated in a spinal cord injury study, in which the degradation-resistant Cdh1-APC substrate Id2 allows axons to grow past the injury site (Yu et al., 2011). Thus, it will be important to determine the regenerative role of Smurf1 and Cdh1 inhibition in CNS injury models. Further elucidation of the Cdh1-APC pathway and in particular its regulation, in which phosphorylation is known to play a role (Huynh et al., 2009), will be important aims of future research that should significantly contribute to our understanding of axon growth suppression and might accelerate the development of regenerative therapies.

Acknowledgements
We thank Drs Nils Brose (MPIem, Göttigen, Germany), Stefan Irniger (University of Göttingen, Germany), Hiroshi Kawabe (MPIem, Göttingen, Germany) and members of the J.S. laboratory for critically reading the manuscript; Pontus Aspenström (Ludwig Institute for Cancer Research, Uppsala, Sweden) for the GST-Rhotekin plasmid; Mostafa Bakti (MPIem, Göttingen, Germany) for providing purified myelin; Azad Bonni (Harvard Medical School, USA) for providing the Cdh1 antibody; J. Silvio Gutkind (NIH, USA) for the Rho and Cdc42 plasmids; Joan Massague for the HA-Smurf1 plasmid; Pumin Zhang (Baylor College of Medicine, TX, USA) for sharing the Cdh1 gene trap mouse line; and Jan Hoeber for assisting in the initial phase of the study.

Funding
This study was supported by the Max Planck Society (J.S.), the German Research Foundation (Deutsche Forschungsgemeinschaft, DFG) (J.S.) and the GGNB (Göttingen Graduate School for Neurosciences and Molecular Biosciences) Excellence Stipend of the University of Göttingen (S.-J.L.).

Competing interests statement
The authors declare no competing financial interests.

Author contributions
M.K. conceived and designed several of the experiments, performed the experiments and analyzed the data. S.-J.L. performed experiments and analyzed data. N.S.-D. performed experiments. J.S. conceived and designed the study, supervised the research, performed experiments and wrote the manuscript.

Supplementary material
Supplementary material available online at
http://dev.biologists.org/lookup/suppl/doi:10.1242/dev.081786/-/DC1

References

Alexandrova, E. M. and Thomsen, G. H. (2006). Smurf1 regulates neural patterning and folding in Xenopus embryos by antagonizing the BMP/Smad1 pathway. *Dev. Biol.* **299**, 398-410.
Almeida, A., Bolaños, J. P. and Moreno, S. (2005). Cdh1/Hct1-APC is essential for the survival of postmitotic neurons. *J. Neurosci.* **25**, 8115-8121.
Aoki, K., Nakamura, T. and Matsuda, M. (2004). Spatio-temporal regulation of Rac1 and Cdc42 activity during nerve growth factor-induced neurite outgrowth in PC12 cells. *J. Biol. Chem.* **279**, 713-719.
Boyer, L., Turchi, L., Desnues, B., Doye, A., Ponzio, G., Mege, J. L., Yamashita, M., Zhang, Y. E., Bertoglio, J., Flatau, G. et al. (2006). CNF1-induced ubiquitylation and proteasome destruction of activated RhoA is impaired in Smurf1–/– cells. *Mol. Biol. Cell* **17**, 2489-2497.
Bryan, B., Cai, Y., Wrighton, K., Wu, G., Feng, X. H. and Liu, M. (2005). Ubiquitination of RhoA by Smurf1 promotes neurite outgrowth. *FEBS Lett.* **579**, 1015-1019.
Cheng, P. L., Lu, H., Shelly, M., Gao, H. and Poo, M. M. (2011). Phosphorylation of E3 ligase Smurf1 switches its substrate preference in support of axon development. *Neuron* **69**, 231-243.
Coso, O. A., Chiariello, M., Yu, J. C., Teramoto, H., Crespo, P., Xu, N., Miki, T. and Gutkind, J. S. (1995). The small GTP-binding proteins Rac1 and Cdc42 regulate the activity of the JNK/SAPK signaling pathway. *Cell* **81**, 1137-1146.
Cui, Y., He, S., Xing, C., Lu, K., Wang, J., Xing, G., Meng, A., Jia, S., He, F. and Zhang, L. (2011). SCF^{FBXL15} regulates BMP signalling by directing the degradation of HECT-type ubiquitin ligase Smurf1. *EMBO J.* **30**, 2675-2689.
Dent, E. W. and Gertler, F. B. (2003). Cytoskeletal dynamics and transport in growth cone motility and axon guidance. *Neuron* **40**, 209-227.
Dickson, B. J. (2001). Rho GTPases in growth cone guidance. *Curr. Opin. Neurobiol.* **11**, 103-110.
Domeniconi, M., Zampieri, N., Spencer, T., Hilaire, M., Mellado, W., Chao, M. V. and Filbin, M. T. (2005). MAG induces regulated intramembrane proteolysis of the p75 neurotrophin receptor to inhibit neurite outgrowth. *Neuron* **46**, 849-855.
Fournier, A. E., Takizawa, B. T. and Strittmatter, S. M. (2003). Rho kinase inhibition enhances axonal regeneration in the injured CNS. *J. Neurosci.* **23**, 1416-1423.
Giger, R. J., Hollis, E. R., 2nd and Tuszynski, M. H. (2010). Guidance molecules in axon regeneration. *Cold Spring Harb. Perspect. Biol.* **2**, a001867.
Glotzer, M., Murray, A. W. and Kirschner, M. W. (1991). Cyclin is degraded by the ubiquitin pathway. *Nature* **349**, 132-138.
Govek, E. E., Newey, S. E. and Van Aelst, L. (2005). The role of the Rho GTPases in neuronal development. *Genes Dev.* **19**, 1-49.
Harper, J. W., Burton, J. L. and Solomon, M. J. (2002). The anaphase-promoting complex: it's not just for mitosis any more. *Genes Dev.* **16**, 2179-2206.

Hata, K., Fujitani, M., Yasuda, Y., Doya, H., Saito, T., Yamagishi, S., Mueller, B. K. and Yamashita, T. (2006). RGMa inhibition promotes axonal growth and recovery after spinal cord injury. *J. Cell Biol.* **173**, 47-58.
Herrero-Mendez, A., Almeida, A., Fernández, E., Maestre, C., Moncada, S. and Bolaños, J. P. (2009). The bioenergetic and antioxidant status of neurons is controlled by continuous degradation of a key glycolytic enzyme by APC/C-Cdh1. *Nat. Cell Biol.* **11**, 747-752.
Hershko, A. and Ciechanover, A. (1998). The ubiquitin system. *Annu. Rev. Biochem.* **67**, 425-479.
Hu, F. and Strittmatter, S. M. (2004). Regulating axon growth within the postnatal central nervous system. *Semin. Perinatol.* **28**, 371-378.
Huber, A. B., Kolodkin, A. L., Ginty, D. D. and Cloutier, J. F. (2003). Signaling at the growth cone: ligand-receptor complexes and the control of axon growth and guidance. *Annu. Rev. Neurosci.* **26**, 509-563.
Huynh, M. A., Stegmüller, J., Litterman, N. and Bonni, A. (2009). Regulation of Cdh1-APC function in axon growth by Cdh1 phosphorylation. *J. Neurosci.* **29**, 4322-4327.
Huynh, M. A., Ikeuchi, Y., Netherton, S., de la Torre-Ubieta, L., Kanadia, R., Stegmüller, J., Cepko, C., Bonni, S. and Bonni, A. (2011). An isoform-specific SnoN1-FOXO1 repressor complex controls neuronal morphogenesis and positioning in the mammalian brain. *Neuron* **69**, 930-944.
Ikeuchi, Y., Stegmüller, J., Netherton, S., Huynh, M. A., Masu, M., Frank, D., Bonni, S. and Bonni, A. (2009). A SnoN-Ccd1 pathway promotes axonal morphogenesis in the mammalian brain. *J. Neurosci.* **29**, 4312-4321.
Juo, P. and Kaplan, J. M. (2004). The anaphase-promoting complex regulates the abundance of GLR-1 glutamate receptors in the ventral nerve cord of C. elegans. *Curr. Biol.* **14**, 2057-2062.
Kawabe, H. and Brose, N. (2011). The role of ubiquitylation in nerve cell development. *Nat. Rev. Neurosci.* **12**, 251-268.
Konishi, Y., Lehtinen, M., Donovan, N. and Bonni, A. (2002). Cdc2 phosphorylation of BAD links the cell cycle to the cell death machinery. *Mol. Cell* **9**, 1005-1016.
Konishi, Y., Stegmüller, J., Matsuda, T., Bonni, S. and Bonni, A. (2004). Cdh1-APC controls axonal growth and patterning in the mammalian brain. *Science* **303**, 1026-1030.
Kranenburg, O., Poland, M., Gebbink, M., Oomen, L. and Moolenaar, W. H. (1997). Dissociation of LPA-induced cytoskeletal contraction from stress fiber formation by differential localization of RhoA. *J. Cell Sci.* **110**, 2417-2427.
Kuczera, T., Stilling, R. M., Hsia, H. E., Bahari-Javan, S., Irniger, S., Nasmyth, K., Sananbenesi, F. and Fischer, A. (2011). The anaphase promoting complex is required for memory function in mice. *Learn. Mem.* **18**, 49-57.
Lasorella, A., Stegmüller, J., Guardavaccaro, D., Liu, G., Carro, M. S., Rothschild, G., de la Torre-Ubieta, L., Pagano, M., Bonni, A. and Iavarone, A. (2006). Degradation of Id2 by the anaphase-promoting complex couples cell cycle exit and axonal growth. *Nature* **442**, 471-474.
Li, M., Shin, Y. H., Hou, L., Huang, X., Wei, Z., Klann, E. and Zhang, P. (2008). The adaptor protein of the anaphase promoting complex Cdh1 is essential in maintaining replicative lifespan and in learning and memory. *Nat. Cell Biol.* **10**, 1083-1089.
Littlepage, L. E. and Ruderman, J. V. (2002). Identification of a new APC/C recognition domain, the A box, which is required for the Cdh1-dependent destruction of the kinase Aurora-A during mitotic exit. *Genes Dev.* **16**, 2274-2285.
Luo, L., Liao, Y. J., Jan, L. Y. and Jan, Y. N. (1994). Distinct morphogenetic functions of similar small GTPases: Drosophila Drac1 is involved in axonal outgrowth and myoblast fusion. *Genes Dev.* **8**, 1787-1802.
McGee, A. W. and Strittmatter, S. M. (2003). The Nogo-66 receptor: focusing myelin inhibition of axon regeneration. *Trends Neurosci.* **26**, 193-198.
Nalepa, G., Rolfe, M. and Harper, J. W. (2006). Drug discovery in the ubiquitin-proteasome system. *Nat. Rev. Drug Discov.* **5**, 596-613.
Ozdamar, B., Bose, R., Barrios-Rodiles, M., Wang, H. R., Zhang, Y. and Wrana, J. L. (2005). Regulation of the polarity protein Par6 by TGFbeta receptors controls epithelial cell plasticity. *Science* **307**, 1603-1609.
Peters, J. M. (2002). The anaphase-promoting complex: proteolysis in mitosis and beyond. *Mol. Cell* **9**, 931-943.
Pfleger, C. M. and Kirschner, M. W. (2000). The KEN box: an APC recognition signal distinct from the D box targeted by Cdh1. *Genes Dev.* **14**, 655-665.
Sarner, S., Kozma, R., Ahmed, S. and Lim, L. (2000). Phosphatidylinositol 3-kinase, Cdc42, and Rac1 act downstream of Ras in integrin-dependent neurite outgrowth in N1E-115 neuroblastoma cells. *Mol. Cell. Biol.* **20**, 158-172.
Sato, Y. and Heuckeroth, R. O. (2008). Retinoic acid regulates murine enteric nervous system precursor proliferation, enhances neuronal precursor differentiation, and reduces neurite growth in vitro. *Dev. Biol.* **320**, 185-198.
Schwab, M. E. (2004). Nogo and axon regeneration. *Curr. Opin. Neurobiol.* **14**, 118-124.
Schwamborn, J. C. and Püschel, A. W. (2004). The sequential activity of the GTPases Rap1B and Cdc42 determines neuronal polarity. *Nat. Neurosci.* **7**, 923-929.
Silies, M. and Klämbt, C. (2010). APC/C(Fzr/Cdh1)-dependent regulation of cell adhesion controls glial migration in the Drosophila PNS. *Nat. Neurosci.* **13**, 1357-1364.
Stegmüller, J. and Bonni, A. (2010). Destroy to create: E3 ubiquitin ligases in neurogenesis. *F1000 Biol. Rep.* **2**, 38.
Stegmüller, J., Konishi, Y., Huynh, M. A., Yuan, Z., Dibacco, S. and Bonni, A. (2006). Cell-intrinsic regulation of axonal morphogenesis by the Cdh1-APC target SnoN. *Neuron* **50**, 389-400.
Stegmüller, J., Huynh, M. A., Yuan, Z., Konishi, Y. and Bonni, A. (2008). TGFbeta-Smad2 signaling regulates the Cdh1-APC/SnoN pathway of axonal morphogenesis. *J. Neurosci.* **28**, 1961-1969.
Stroschein, S. L., Bonni, S., Wrana, J. L. and Luo, K. (2001). Smad3 recruits the anaphase-promoting complex for ubiquitination and degradation of SnoN. *Genes Dev.* **15**, 2822-2836.
Tajima, Y., Goto, K., Yoshida, M., Shinomiya, K., Sekimoto, T., Yoneda, Y., Miyazono, K. and Imamura, T. (2003). Chromosomal region maintenance 1 (CRM1)-dependent nuclear export of Smad ubiquitin regulatory factor 1 (Smurf1) is essential for negative regulation of transforming growth factor-beta signaling by Smad7. *J. Biol. Chem.* **278**, 10716-10721.
van Roessel, P., Elliott, D. A., Robinson, I. M., Prokop, A. and Brand, A. H. (2004). Independent regulation of synaptic size and activity by the anaphase-promoting complex. *Cell* **119**, 707-718.
Vohra, B. P., Fu, M. and Heuckeroth, R. O. (2007). Protein kinase Czeta and glycogen synthase kinase-3beta control neuronal polarity in developing rodent enteric neurons, whereas SMAD specific E3 ubiquitin protein ligase 1 promotes neurite growth but does not influence polarity. *J. Neurosci.* **27**, 9458-9468.
Wan, L., Zou, W., Gao, D., Inuzuka, H., Fukushima, H., Berg, A. H., Drapp, R., Shaik, S., Hu, D., Lester, C. et al. (2011). Cdh1 regulates osteoblast function through an APC/C-independent modulation of Smurf1. *Mol. Cell* **44**, 721-733.
Wang, K. C., Kim, J. A., Sivasankaran, R., Segal, R. and He, Z. (2002). P75 interacts with the Nogo receptor as a co-receptor for Nogo, MAG and OMgp. *Nature* **420**, 74-78.
Wang, H. R., Zhang, Y., Ozdamar, B., Ogunjimi, A. A., Alexandrova, E., Thomsen, G. H. and Wrana, J. L. (2003). Regulation of cell polarity and protrusion formation by targeting RhoA for degradation. *Science* **302**, 1775-1779.
Winzeler, A. M., Mandemakers, W. J., Sun, M. Z., Stafford, M., Phillips, C. T. and Barres, B. A. (2011). The lipid sulfatide is a novel myelin-associated inhibitor of CNS axon outgrowth. *J. Neurosci.* **31**, 6481-6492.
Wong, S. T., Henley, J. R., Kanning, K. C., Huang, K. H., Bothwell, M. and Poo, M. M. (2002). A p75(NTR) and Nogo receptor complex mediates repulsive signaling by myelin-associated glycoprotein. *Nat. Neurosci.* **5**, 1302-1308.
Yamashita, M., Ying, S. X., Zhang, G. M., Li, C., Cheng, S. Y., Deng, C. X. and Zhang, Y. E. (2005). Ubiquitin ligase Smurf1 controls osteoblast activity and bone homeostasis by targeting MEKK2 for degradation. *Cell* **121**, 101-113.
Yi, J. J. and Ehlers, M. D. (2007). Emerging roles for ubiquitin and protein degradation in neuronal function. *Pharmacol. Rev.* **59**, 14-39.
Yiu, G. and He, Z. (2006). Glial inhibition of CNS axon regeneration. *Nat. Rev. Neurosci.* **7**, 617-627.
Yoneda, Y., Hieda, M., Nagoshi, E. and Miyamoto, Y. (1999). Nucleocytoplasmic protein transport and recycling of Ran. *Cell Struct. Funct.* **24**, 425-433.
Yu, P., Zhang, Y. P., Shields, L. B., Zheng, Y., Hu, X., Hill, R., Howard, R., Gu, Z., Burke, D. A., Whittemore, S. R. et al. (2011). Inhibitor of DNA binding 2 promotes sensory axonal growth after SCI. *Exp. Neurol.* **231**, 38-44.

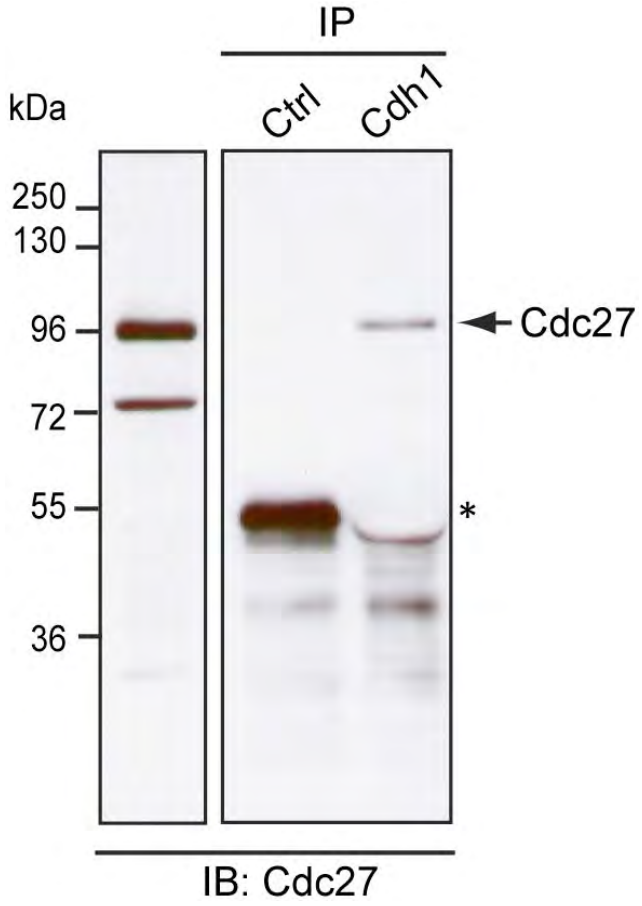

Fig. S1. Cdh1 associates with Cdc27. P9 brain lysates subjected to immunoprecipitation using control serum or Cdh1 antibody followed by immunoblotting with Cdc27 antibody. Arrow indicates Cdc27 and asterisk indicates IgG_H.

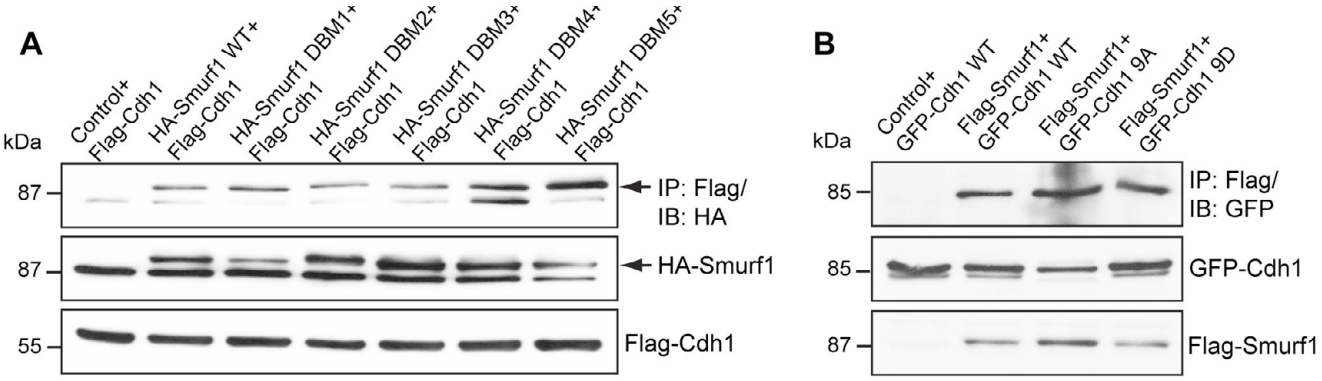

Fig. S2. Co-immunoprecipitation analyses of Cdh1 and Smurf1. (**A**) Lysates of 293T cells transfected with Flag-Cdh1 and control pCMV5 or HA-Smurf1 WT or HA-Smurf1 DBM1-5 plasmids were subjected to immunoprecipitation with the Flag antibody followed by immunoblotting with HA antibody. Arrows indicate HA-Smurf1. (**B**) Lysates of 293T cells transfected with control pCMV5 or the Flag-Smurf1 expression plasmid together with the Cdh1 WT, Cdh1 9A (hypophosphorylated form) or the Cdh1 9D (hyperphosphorylated form) plasmid were subjected to immunoprecipitation with Flag antibody followed by immunoblotting with GFP antibody.

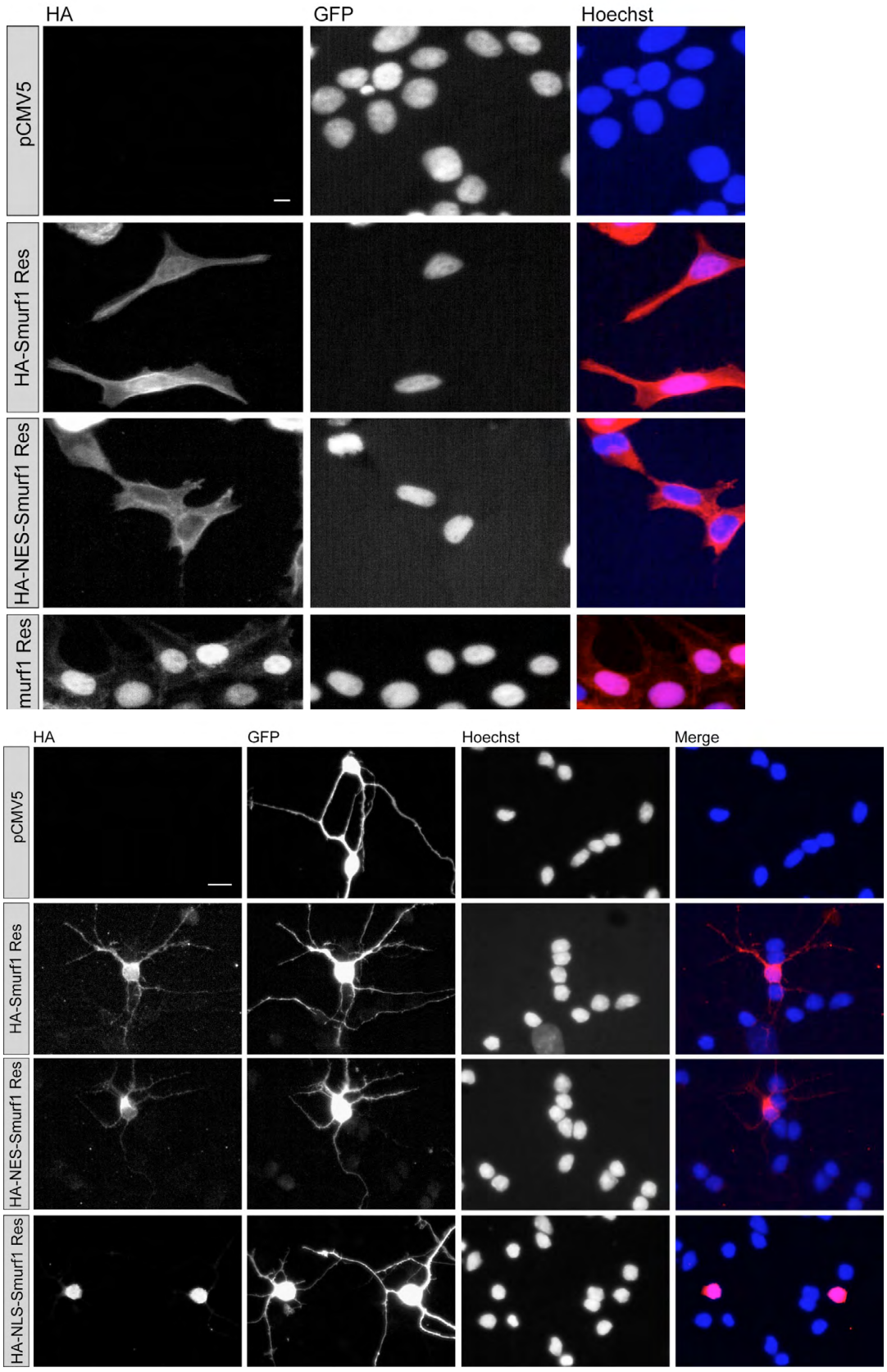

Fig. S3. Subcellular localization of Smurf1 mutants. (**A**) 293T cells transfected with control vector pCMV5, HA-Smurf1-Res, HA-NES-Smurf1-Res or HA-NLS-Smurf1-Res plasmids were subjected to immunocytochemistry using HA antibody and Hoechst 33258 staining. (**B**) Granule neurons transfected at DIV 1 with control vector pCMV5, HA-Smurf1-Res, HA-NES-Smurf1-Res or HA-NLS-Smurf1-Res plasmids together with the GFP plasmid were fixed at DIV 3 and subjected to double immunostaining using GFP and HA antibodies and Hoechst 33258 staining. Asterisks indicate soma. Scale bars: 10 μm.

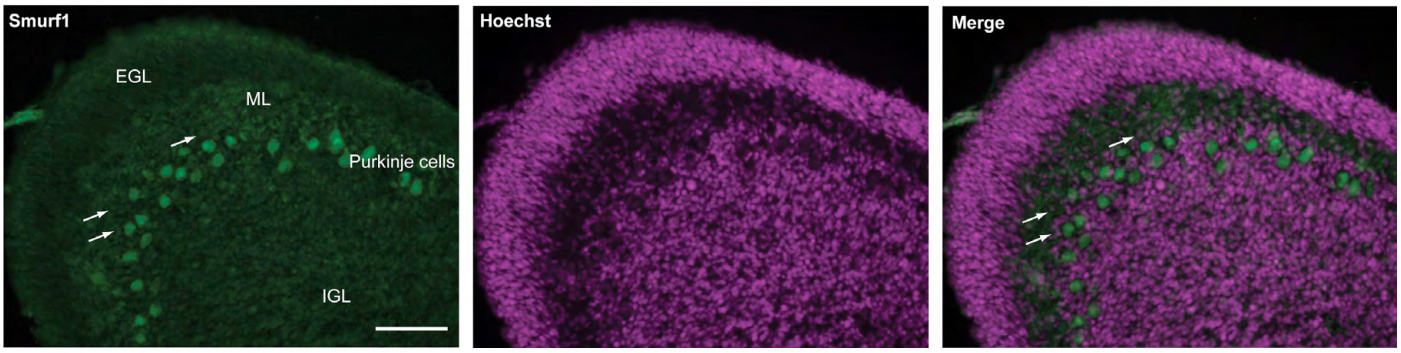

Fig. S4. Smurf1 is expressed in migrating granule neurons and Purkinje cells. Sagittal sections of P9 cerebella subjected to immunostaining with Smurf1 antibody and counterstained with DNA dye bisbenzimide Hoechst 33258. Arrows indicate Smurf1-positive neurons in the molecular layer. EGL, external granular layer; ML, molecular layer; IGL, internal granular layer. Scale bar: 50 μm.

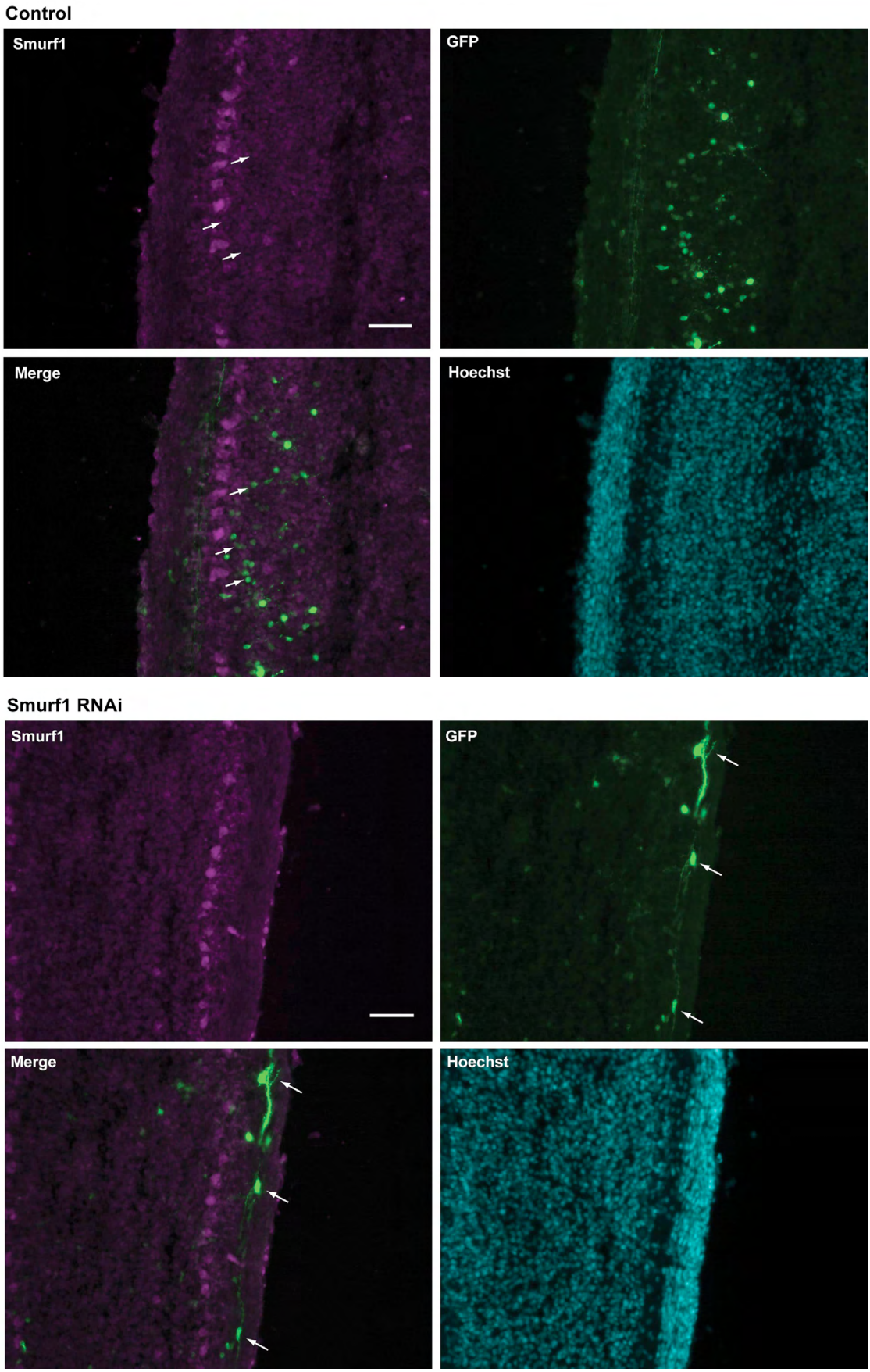

Fig. S5. Smurf1 knockdown neurons stall at the EGL/ML border. Coronal sections of (**A**) control and (**B**) Smurf1 RNAi-electroporated cerebella were subjected to Smurf1 and GFP double immunostaining and DNA counterstain. Arrows in A indicate Smurf1-positive transfected neurons in the internal granular layer; arrows in B indicate transfected Smurf1 knockdown neurons in the external granular layer. Scale bars: 50 μm.

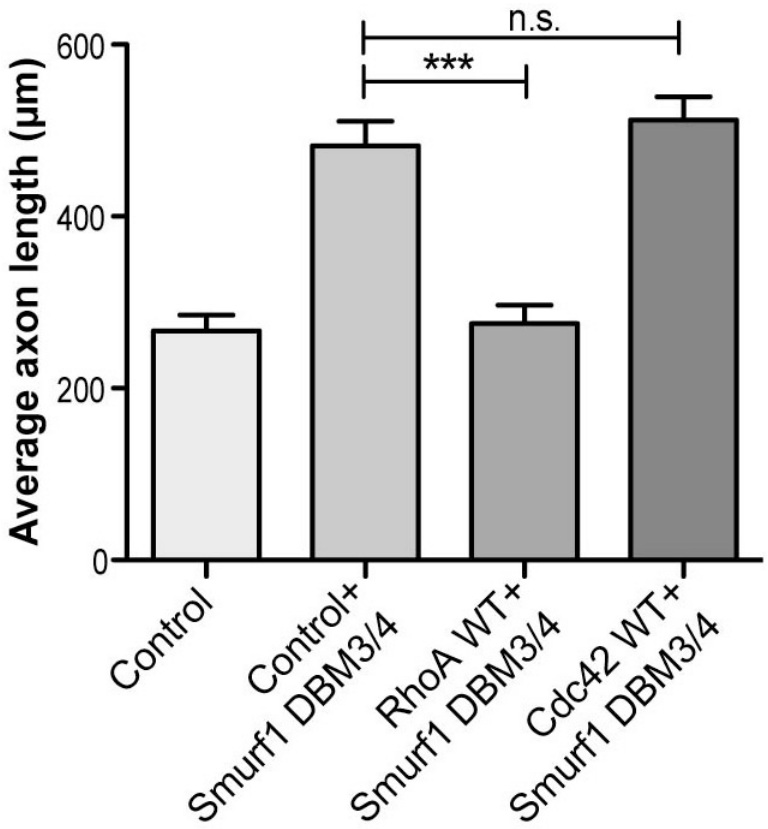

Fig. S6. Cdc42 does not counteract Smurf1 DBM3/4-induced axon growth. Granule neurons were transfected at DIV 0 with control vectors pCMV5 and pCEFL, Smurf1 DBM3/4 expression plasmid together with pCEFL or plasmids encoding RhoA WT or Cdc42 WT and analyzed at DIV 3 as in Fig. 1A. A total of 289 neurons were measured. ANOVA, ***P<0.0001; n.s., non-significant; mean + s.e.m.

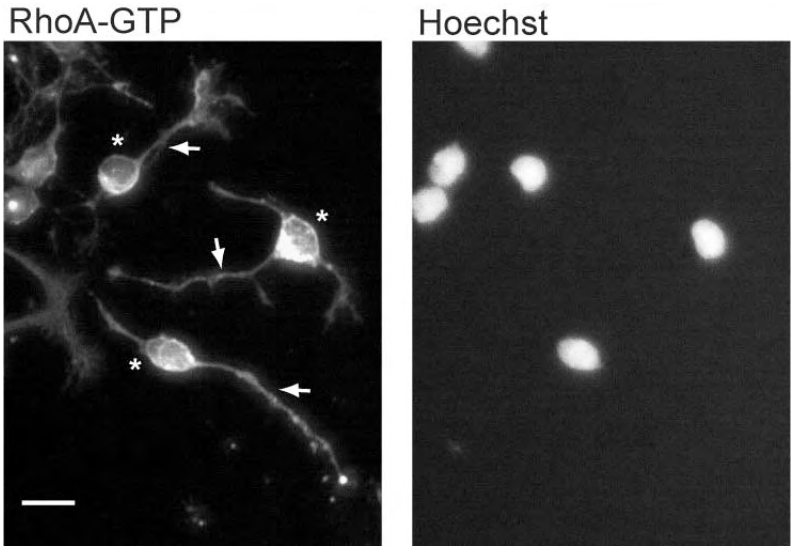

Fig. S7. Active RhoA localizes to the cytoplasmic compartment in neurons. Cerebellar granule neurons at DIV 2 were subjected to immunocytochemistry with the active RhoA antibody and the nuclear dye bisbenzimide Hoechst 33258. Arrows and asterisks indicate axons and soma, respectively. Scale bar: 10 µm.

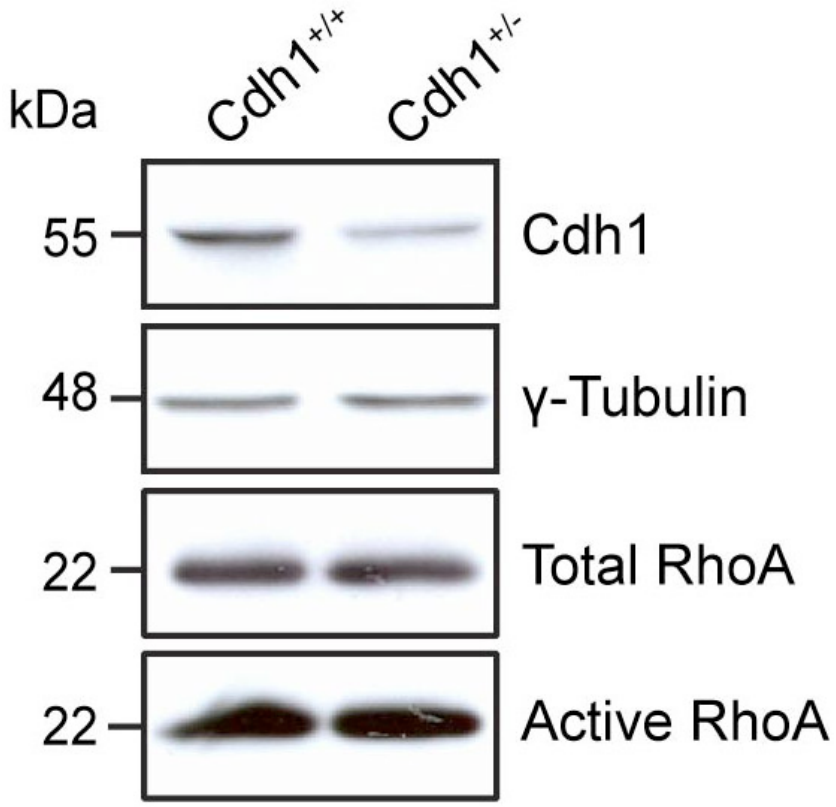

Fig. S8. No change in total and active RhoA in the brain of Cdh1 heterozygous animals. Cerebellar lysates of week (W) 10 *Cdh1*$^{+/+}$ and *Cdh1*$^{+/-}$ mice were immunoblotted with RhoA and Cdh1 antibodies. γ-tubulin served as loading control. For detection of active RhoA, the lysates were subjected to GST pulldown using GST-Rhotekin-conjugated beads and immunoblotted using RhoA antibody.

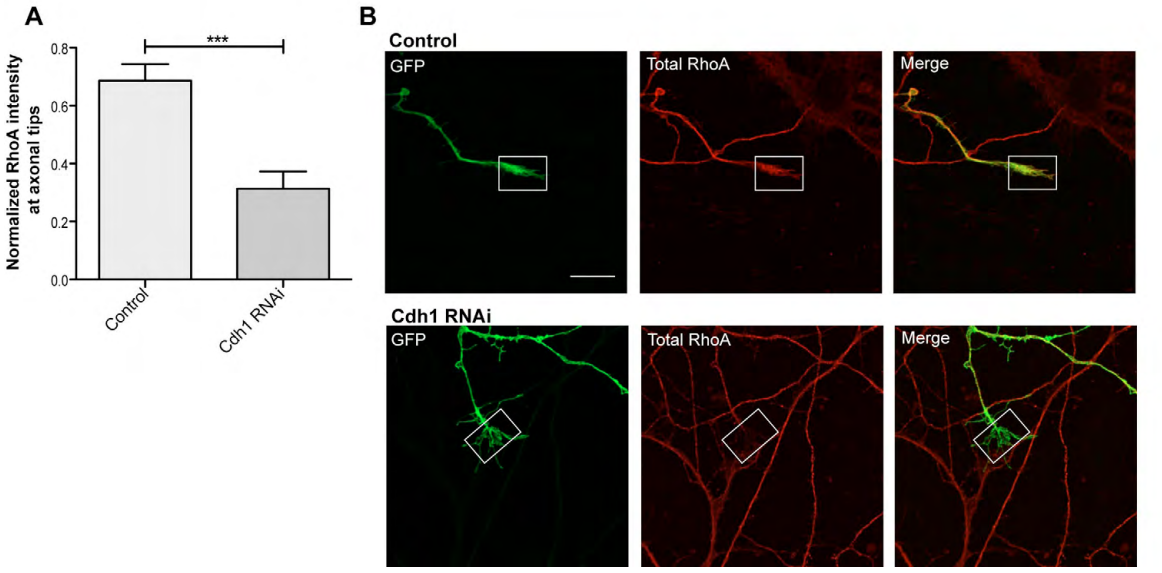

Fig. S9. Total RhoA levels are reduced at axonal tips in Cdh1 knockdown neurons. (**A**) Hippocampal neurons transfected at DIV 2 with control U6 and Cdh1 RNAi plasmids together with the GFP plasmid were fixed at DIV 6 and subjected to double immunostaining using GFP and RhoA antibodies and Hoechst 33258 staining. The intensity of RhoA staining at axon tips and axons was determined by the mean gray values and normalized to that of GFP. Normalized RhoA intensity at the axon tips was further normalized to that in the axons. A total of 28 neurons were measured. *t*-test, ***P<0.0001; mean + s.e.m. (**B**) Representative images of transfected neurons in A. Box indicates region of interest. Scale bar: 5 μm.

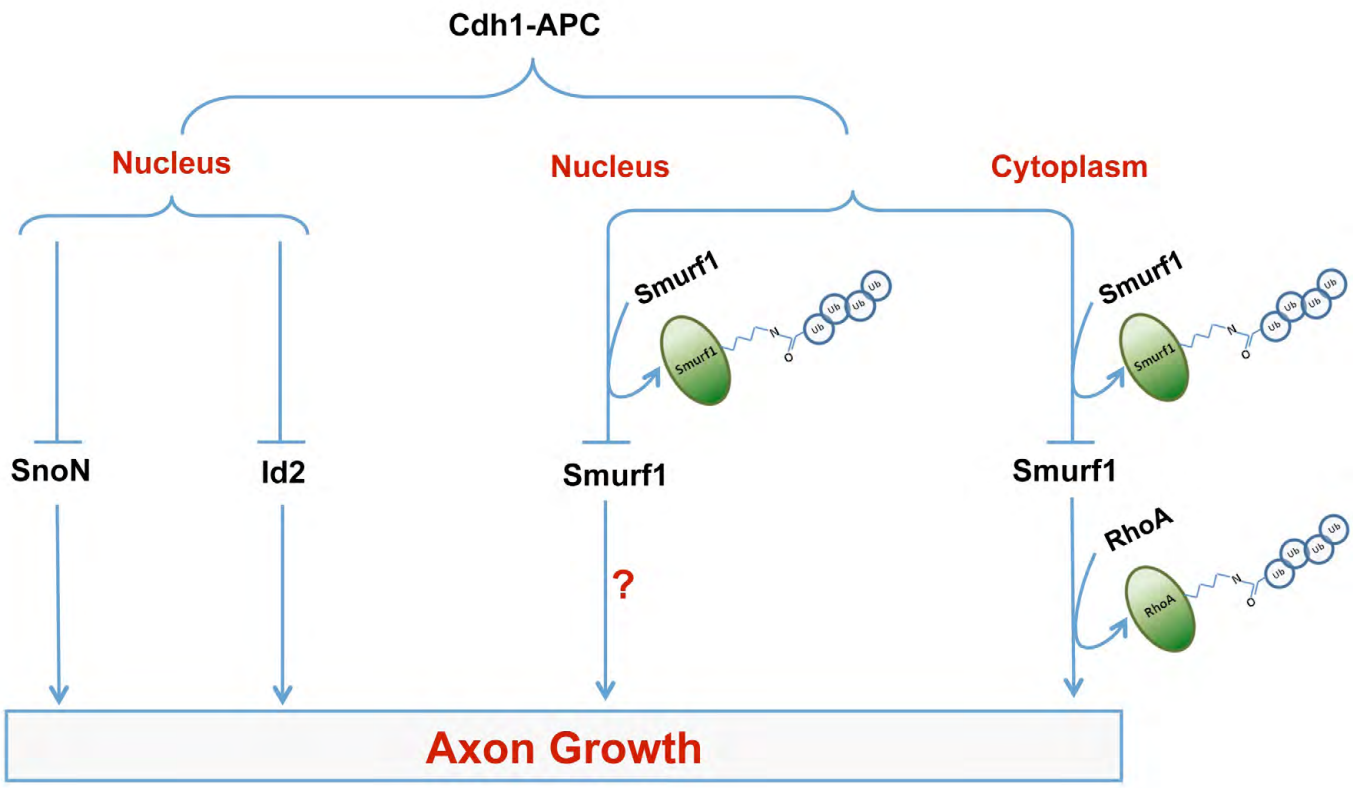

Fig. S10. Model of the Cdh1-APC pathway of axon growth regulation. The E3 ubiquitin ligase Cdh1-APC targets the transcriptional regulators SnoN and Id2 (Lasorella et al., 2006; Stegmüller et al., 2006) and the E3 ligase Smurf1 for ubiquitylation and proteasomal degradation and thus negatively regulates axon growth. Whereas SnoN and Id2 reside in the nucleus to control axon growth, Smurf1 is required both in the nucleus and cytoplasm to regulate axon growth. RhoA is the relevant target of Smurf1 in its cytoplasmic control of axon growth and operates in the Cdh1-APC/Smurf1 axis.